

Eukaryotic influence on the oceanic biological carbon pump in the Scotia Sea as revealed by 18S rRNA gene sequencing of suspended and sinking particles

Manon T. Duret ^{1*}, Richard S. Lampitt,² Phyllis Lam¹

¹Ocean and Earth Science, University of Southampton, Southampton, United Kingdom

²National Oceanography Centre, Southampton, United Kingdom

Abstract

Suspended marine particles constitute most of the particulate organic matter pool in the oceans, thereby providing substantial substrates for heterotrophs, especially in the mesopelagic. Conversely, sinking particles are major contributors to carbon fluxes defining the strength of the biological carbon pump (BCP). This study is the first to investigate the differential influence of eukaryotic communities to suspended and sinking particles, using 18S rRNA gene sequencing on particles collected with a marine snow catcher in the mixed layer and upper mesopelagic of the Scotia Sea, Southern Ocean. In the upper mesopelagic, most eukaryotic phytoplankton sequences belonged to chain-forming diatoms in sinking particles and to prymnesiophytes in suspended particles. This suggests that diatom-enriched particles are more efficient in carbon transfer to the upper mesopelagic than those enriched in prymnesiophytes in the Scotia Sea, the latter more easily disintegrating into suspended particles. In the upper mesopelagic, copepods appeared most influential on sinking particles whereas soft-tissue metazoan sequences contributed more to suspended particles. Heterotrophic protists and fungi communities were distinct between mixed layer and upper mesopelagic, implying that few protists ride along sinking particles. Furthermore, differences between predatory flagellates and radiolarians between suspended and sinking particles implied different ecological conditions between the two particles pools, and roles in the BCP. Molecular analyses of sinking and suspended particles constitute powerful diagnostic tools to study the eukaryotic influence on the BCP in a more holistic manner compared to classic carbon export studies focusing on sinking particles.

The oceanic biological carbon pump (BCP) corresponds to the processes by which organic matter produced by phytoplankton's photosynthesis in the sunlit epipelagic ocean (upper ~ 100 m) is exported to depth, thereby sequestering atmospheric carbon in the mesopelagic (~ 100–1000 m) and deeper ocean (Turner 2015). This downward export of organic matter removes each year more than 10 billion tons of carbon from the epipelagic (Buesseler and Boyd 2009), representing 5% to 25% of the euphotic photosynthetic primary production reaching the mesopelagic (De La Rocha and Passow 2007). Most of this

autochthonous carbon flux occurs in the form of particulate organic matter (POM). POM consists of a combination of different materials such as fecal pellets, living and nonliving microbial cells and fragments of cells, empty larvacean houses—all of which, if not occurring on their own, can be incorporated into large aggregated entities known as marine snow. In coastal systems, some allochthonous POM, such as POM originating from river runoffs, can also constitute sinking particles. The nature of these sinking particles depends largely on the structure of phytoplankton community (Korb et al. 2012) and heterotrophic community members, including mesozooplankton (> 200 μm) (Steinberg and Landry 2017) and heterotrophic microbes (prokaryotes and unicellular eukaryotes or protists) (Worden et al. 2015).

Heterotrophic communities alter the BCP efficiency, either (1) negatively by reducing carbon export owing to remineralization processes that release carbon dioxide (CO₂) and inorganic nutrients (Cho and Azam 1988; Smith et al. 1992; Kiørboe and Jackson 2001; Steinberg et al. 2008; Collins et al. 2015); or (2) positively by enhancing carbon export to depth. Mesozooplankton can indeed lead to an increase of particle

*Correspondence: m.t.duret@soton.ac.uk

This is an open access article under the terms of the Creative Commons Attribution License, which permits use, distribution and reproduction in any medium, provided the original work is properly cited.

Additional Supporting Information may be found in the online version of this article.

Special Issue: Linking Metagenomics to Aquatic Microbial Ecology and Biogeochemical Cycles. Edited by: Hans-Peter Grossart, Ramon Massana, Katherine McMahon and David A. Walsh.

export by grazing on phytoplankton cells and other small particles, subsequently repackaging them into larger fecal pellets ($\geq 50 \mu\text{m}$ depending on the species) (Stamieszkin et al. 2017) which can then sink faster to depth (Atkinson et al. 2001; Giesecke et al. 2010; Ebersbach et al. 2011), although not all fecal pellets sink (Lampitt et al. 1990). Additionally, vertical migration of mesozooplankton may lead to the active transfer of organic matter from one depth to another, as they feed on POM in the epipelagic and release fecal pellets and dissolved organic matter (DOM) at greater depths (Steinberg et al. 2000). Examples include decapods (Pakhomov et al. 2018), copepods (Cavan et al. 2015; Yebra et al. 2018), and gelatinous zooplankton (Allredge 1976; Wilson et al. 2008). Conversely, they can release DOM and break sinking particles into smaller pieces that remain in suspension in the water column (suspended particles) (De La Rocha and Passow 2007) via sloppy feeding (Strom et al. 1997). The proportion of suspended particles originating from the disaggregation of sinking particles is currently unknown (Lam and Marchal 2015), as it is governed by complex abiotic and biotic processes such as those mentioned above, as well as feeding behaviors of micro- and nanozooplankton (protists 20–200 and 2–20 μm , respectively) (Ploug and Grossart 2000; Poulsen and Iversen 2008).

Heterotrophic protists, such as flagellates and ciliates, are enriched in large sinking particles relative to surrounding waters (Simon et al. 2002), even in the bathypelagic ocean (~ 1000–4000 m) (Bochdansky et al. 2017). Micro- and nanozooplankton consume ~ 60% of the daily phytoplankton primary production (Calbet and Landry 2004; Schmoker et al. 2013). By doing so, they can contribute to carbon export by producing “minipellets” (3–50 μm fecal pellets) when dense enough to sink (Gowing and Silver 1985). However, they also allow organic matter to enter the microbial loop, thereby lengthening the “food chain” while reducing carbon export (Pomeroy and Wiebe 1988; Legendre and Le Fevre 1995; Legendre and Rassoulzadegan 1996). Although studies have focused on differences between various sizes of freely suspended and particle-associated protists—for example, cutoff sizes at 30 μm (Duret et al. 2015; Bochdansky et al. 2017) and 1.6 μm (Parris et al. 2014), these communities remain largely understudied (Edgcomb 2016; Caron 2017). Similarly, fungal communities in open-ocean and polar systems remain poorly known (Grossart et al. 2019), although studies have shown their importance in the degradation of marine snow (Bochdansky et al. 2017).

While heterotrophs lead to a decrease of sinking particles concentration of with depth (Martin et al. 1987; Francois et al. 2002), the quantity of suspended particles remains constant with depth, presenting an organic carbon content generally at two or more orders of magnitude higher than that of sinking particles (Bishop et al. 1977; Bacon et al. 1985; Verdugo et al. 2004; Riley et al. 2012; Giering et al. 2014; Baker et al. 2017; Cavan et al. 2017). Especially in the mesopelagic, suspended particles constitute major organic carbon substrates for

heterotrophs, including microbes (Baltar et al. 2009, 2010; Herndl and Reinthaler 2013) and micronekton (e.g., fish, cephalopods, and crustaceans) (Gloeckler et al. 2017). Like sinking particles, they are hotspots for microbial activity (Bochdansky et al. 2010) and diversity (Duret et al. 2018). However, most studies on particle-associated microbial communities so far have focused on sinking particles, and primarily on prokaryotes (e.g., Delong et al. 1993; López-Pérez et al. 2012; Crespo et al. 2013; Mestre et al. 2017).

The main reason behind this knowledge gap is owed to the fact that conventional sampling methodologies used for marine microbial communities are unable to distinguish between suspended and sinking particles. They either collect a mixture of both particle pools in unknown proportions (e.g., size-fractionated filtration of seawater) or collect mainly large sinking particles (e.g., sediment traps) (McDonnell et al. 2015). The marine snow catcher (MSC) (Lampitt et al. 1993) is a large water sampler that uses sinking velocity to differentiate suspended from sinking particles originating from the same water sample. This is the first study to investigate the differential contribution of eukaryotic communities in sinking and suspended particles collected with an MSC using 18S rRNA gene amplicon sequencing—either as direct residents within particles or as fragments of dead organisms.

The 18S rRNA gene amplicon sequencing has been used to investigate eukaryotic plankton taxonomic communities distribution and their inferred preferential ecological niches at large scales (e.g., Pernice et al. 2013, 2016; de Vargas et al. 2015), as well as in specific oceanic environments (e.g., Sauvadet et al. 2010; Orsi et al. 2012). Comparing the taxonomic composition of eukaryotic communities associated with sinking particles in the mixed layer from sinking particles in the upper mesopelagic would help assessing the continuity of particle composition with depth, and thus identifying key contributors to carbon export. Furthermore, comparing the taxonomic composition of sinking particles in the mixed layer from suspended particles in the upper mesopelagic would inform us on particle dynamics and the influence of sinking particle disaggregation on suspended particle composition (Lam and Marchal 2015). More specifically, our objectives were to assess (1) which eukaryotic phytoplankton taxa are the most efficient in particulate carbon export to the mesopelagic in the Scotia Sea, (2) what metazoan and eukaryotic phytoplankton taxa contribute to sinking and suspended particles in the upper mesopelagic, and (3) if the heterotrophic protist and fungal communities in the two particle pools differ in the upper mesopelagic, such that they have different roles in particle attenuation and the BCP.

Materials

Study site

Sampling took place during the austral summer 2014 (15 November to 12 December) on-board the *RRS James Clark*

Ross (cruise JR304). In the Scotia Sea, four stations of contrasting nutrient regimes and surface productivity were sampled, including two low-productivity stations—ICE (59.9624°S, 46.1597°W) and P2 (55.2484°S, 41.2640°W)—and two additional higher productive stations—P3 (52.8121°S, 39.9724°W) and UP (52.06018°S, 39.1994°W). Surface particulate organic carbon (POC) data are presented on a map constructed with the Ocean Data View software (<https://odv.awi.de>) using the mean values for December 2014 deduced from ocean color by the MODIS satellite (<http://oceancolor.gsfc.nasa.gov/cgi/l3>) (Fig. 1).

Temperature, oxygen concentration, and chlorophyll *a* concentration based on fluorescence measurements were measured with a conductivity-temperature-depth device (CTD Seabird 9Plus with SBE32 carousel) (Fig. S1). POC concentrations were measured by and are presented in Belcher et al. (2016b) from samples collected with an MSC on the same cruise.

Particle sampling

Particles were collected with an MSC deployed at the base of the mixed layer and in the upper mesopelagic (~ 110 m below the deep chlorophyll maximum). Both deployments occurred within ~ 30 min of each other. The former depth was chosen because it usually corresponds to a peak in particle abundance in this region (Belcher et al. 2016b). The latter

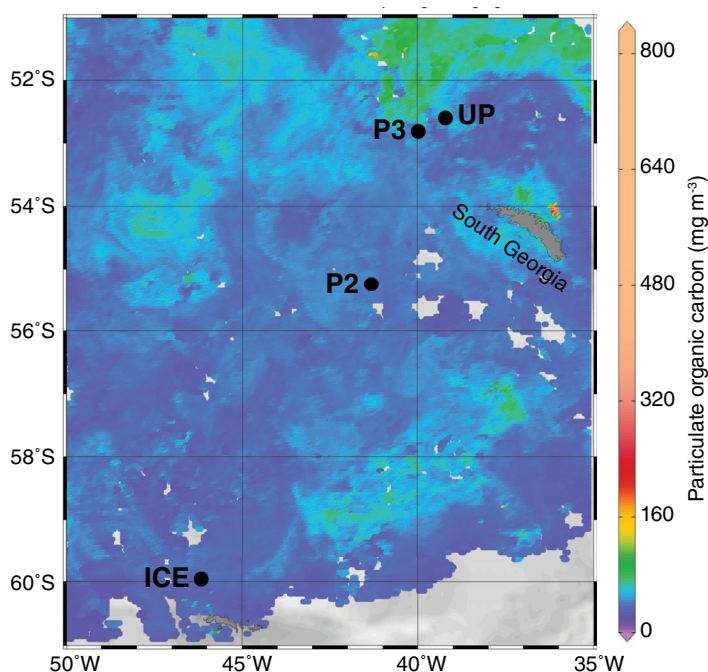


Fig. 1. Location of sampling sites on a map of surface particulate organic carbon. The map was constructed on Ocean Data View using data from NASA Ocean Color 9 km resolution level 3 browser. The surface particulate organic carbon data were corrected by D. Stramski 2007 method (version 443/555) and correspond to a 32-d composition (17 Nov 2014–18 Dec 2014).

depth was chosen as it is usually where the sharpest decline in particle concentration with depth is observed, and where transfer efficiency of the BCP is usually determined (Buesseler and Boyd 2009). These depths were defined using fluorescence profiles taken during CTD cast deployed maximum 4 hr prior to MSC deployments (Fig. S1).

After its retrieval from the desired depth, the MSC is left undisturbed on the ship's deck for 2 hr. This period allows sinking particles to settle at the bottom of the sampler (MSCB) while suspended particles remain in suspension in the upper part (MSCU), as described and illustrated in Riley et al. (2012) and Duret et al. (2018). Water samples are collected from the MSCU followed by the MSCB. Sinking particles are defined here as the particles that have sunk to the MSCB after 2 hr (average sinking velocity $\geq 12 \text{ m d}^{-1}$) and include both slow- and fast-sinking particles (Riley et al. 2012). Particles remaining in suspension in the MSCU are considered suspended. Both sinking and suspended particles consisted of a mixture of single free-living cells and cells associated with particles or aggregates. Each MSCU sample was subsequently size fractionated to further separate collected particles into size-classes.

Suspended particles were sampled by sequentially filtering ~ 10 L of seawater collected from the MSCU through (1) a 100 μm pore-size nylon filter (47 mm diameter, Millipore), (2) a 10 μm pore-size polycarbonate membrane filter (47 mm diameter, Millipore), and (3) a 0.22 μm pore-size Sterivex cartridge filter (Millipore) driven by a peristaltic pump. Sinking particles were collected by gravity-filtering ~ 1.5 L of seawater collected from the MSCB onto a 10 μm pore-size polycarbonate membrane filter. Both filtering steps were performed in under 1 hr, and filters were subsequently incubated with RNAlater (Ambion™, Thermo Fisher Scientific) for 12 hr at 4°C, prior to being stored at -80°C until further processing onshore. In total, four particle fractions were collected at each station and at each depth: (1) suspended particles 0.22–10 μm (referred to as SS0.22), (2) 10–100 μm (SS10), (3) $\geq 100 \mu\text{m}$ (SS100), and (4) sinking particles $\geq 10 \mu\text{m}$ (SK10).

DNA extraction and sequencing

Nucleic acids were recovered from the filters using a ToTALLY RNA kit (Ambion™, Thermo Fisher Scientific) followed by a DNA extraction step as described in Lam et al. (2011)—though only DNA extracts were considered in this study. Extracted DNA was further purified with a Wizard DNA clean-up system (Promega) following manufacturer's recommendations.

Amplicon sequencing of eukaryotic 18S rDNA V4 region was performed according to Hadziavdic et al. (2014) and following the Illumina "16S metagenomic sequencing library preparation" protocol. The primer set F-574 (5'-GCGGTAATTCAGCTCCAA-3') and R-952 (5'-TTGGCAAATGCTTTCGC-3'; 378 bp), including overhang adapters (respectively 5'-TCGTCGGCAGCGTCAGATGTGTATAAGAGACAG-3' and 5'-GTCTCGTGGGCTCGGAGATGTGTATAAGAGACAG-3'), was used for

the first PCR, with each reaction comprising 2.5 μL of purified DNA extract, 5 μL of each forward and reverse primers, 12.5 μL of 2X proofreading polymerase Kapa Hifi Hotstart ready mix (Kapa Biosystems). The PCR conditions followed were: 95°C for 3 min, 25 cycles of 95°C for 30 s, 55°C for 30 s, and 72°C for 30 s, and finally 72°C for 5 min. These amplicons were subsequently used as templates for an indexing PCR for the overhangs to be linked to Illumina sequencing adapters and indices (Nextera XT Index Primer 1, i7, and Primer 2, i5) for downstream sequencing. Each PCR reaction included 5 μL of amplicon from the first PCR, 5 μL of each Nextera primers and 10 μL of PCR-grade water, 25 μL 2X Kapa Hifi Hotstart ready mix, and followed PCR conditions of 95°C for 3 min, 10 cycles of 95°C for 30 s, 55°C for 30 s, and 72°C for 30 s, and a final extension at 72°C for 5 min. For the samples showing a total amount of extracted DNA less than 12.5 ng (ICE SS10 mixed layer, UP and P3 SS100 upper mesopelagic), a nested PCR approach was applied. That step included an additional amplification with the universal 18S rDNA primers set prior to the two-step PCR described above. This procedure caused little variation in the OTU composition and structure of microbial communities, as evidenced in Duret et al. (2018). After each PCR round, amplicons were purified with the Agencourt AMPure XP PCR clean-up kit (Beckman Coulter) following manufacturer's recommendations. The quality of purified amplicons was assessed with a DNA7500 Kit read on a 2100 Bioanalyser (Agilent Technologies) and the quantity measured with a Qubit dsDNA High-Sensitivity assay kit (Invitrogen™, Thermo Fisher Scientific). Purified amplicons were pooled at equimolar concentrations (4 nM each) for the library preparation using a Nextera XT DNA kit (Illumina) following manufacturer's recommendations and included 5% PhiX. Finally, the amplicons were sequenced with an Illumina MiSeq sequencing system (M02946, Illumina) using a MiSeq Reagent 600-cycle Kit v3 (Illumina).

Bioinformatics

Raw sequences were demultiplexed and their adapters trimmed using the MiSeq Control software (v2.5.0.5, Illumina) directly after sequencing. The quality of demultiplexed raw read pairs was checked with FastQC (v0.11.4; Babraham Bioinformatics). Forward and reverse reads were merged with the PANDAseq assembler software (v 2.8) (Masella et al. 2012) using the default parameters (simple Bayesian algorithm for assembly), and a maximum read length of 500 bp and Phred33 quality score of 0.8. OTU clustering was subsequently performed under QIIME (MacQIIME v 1.9.1_20150604) (Caporaso et al. 2010) after all libraries were compiled into a single FASTA file using the *multiple_split_libraries_fastq.py* function. Clustering was performed using the open reference function *pick_open_reference_otus.py* using default parameters (UCLUST algorithm for OTU picking) using a minimum sequence identity of 97% against the SSU Silva database (v 128) (Quast et al. 2013), and against the PR² database (v 4.11.1) (Guillou et al. 2012) for heterotrophic protists and fungi. Singleton OTUs were discarded.

Based on taxonomic affiliation and/or physiological information, OTUs were divided into several categories for individual analyses and further discussions: phytoplankton, metazoans, dinoflagellates, choanoflagellates, *Syndiniales*, ciliates, rhizarians, and fungi. Relative abundances of specific OTUs were normalized to the total number of sequences in the category they belong to. This classification would have inadvertently included some ambiguities, such as the classification of certain mixotrophs/heterotrophs in the phytoplankton category (e.g., heterotrophic *Stramenopiles*). Because high-throughput amplicon sequencing of the 18S rRNA gene is subject to PCR biases, it is important to note that relative abundances do not represent absolute quantities. Organisms with high gene copy numbers and DNA contents per cell would disproportionately be favored (Zhu et al. 2005), leading to their overrepresentation (Medinger et al. 2010). Nonetheless, it is informative to compare relative abundances of specific taxa presenting similar copy numbers of the 18S rRNA gene (Gong et al. 2013), which was the primary purpose of the analyses presented in this study.

Statistical analyses

The canonical correspondence analysis (CCA) and permutational multivariate analyses of variance (PERMANOVA) were performed on the rarefied data set and were used to investigate the significance of environmental and inherent sampling factors responsible for community composition variability. The similarity percent analysis (SIMPER) was based on the Bray-Curtis dissimilarity distance of OTU composition and was used to investigate the differences between communities associated with the various particle fractions.

Taxa enrichments in the upper mesopelagic relative to sinking particles (SK10) in the mixed layer were calculated according to the following Eq. 1:

$$\text{Enrichment} = \log_2 \left(\frac{\text{RA}_{\text{sample UM}}}{\text{RA}_{\text{SK10 ML}}} \right) \quad (1)$$

where $\text{RA}_{\text{SK10 ML}}$ is the relative abundance of the taxa in SK10 mixed layer and $\text{RA}_{\text{sample UM}}$ is the relative abundance of the same taxa in the compared sample in the upper mesopelagic. Therefore, negative values indicate an enrichment within mixed layer SK10 while positive values indicate an enrichment within the compared sample.

Analyses were performed with the R statistics software (<http://www.r-project.org>), using features of the *vegan* package. Statistical analyses were performed on the data set rarefied to the smallest library size, either at a considered station and depth or overall (as would be indicated). For the calculation of SIMPER and the proportions of shared/unique OTUs, the data set was rarefied to the smallest library size in a considered station ($n = 16,127$ sequences for ICE; 29,119 for P2; 6,055 for P3 and 28,937 for UP). Multivariate analyses comparing samples from all stations (CCA and PERMANOVA) were performed on the data set rarefied to the smallest library size ($n = 3,976$ sequences/library).

Results and discussion

Sequencing statistics

A total of 2,517,165 V4 18S rDNA paired-ends reads were recovered from all four particle fractions (suspended particles 0.22–0 μm [SS0.22], 10–100 μm [SS10], and $\geq 100 \mu\text{m}$ [SS100], as well as sinking particles $\geq 10 \mu\text{m}$ [SK10]). After sequence trimming, pairing and merging, and separation from meta-zoan sequences, a total of 1,533,266 protist sequences remained with an average length of 450 bp ($29,852 \pm 22,428$ sequences/library) (Fig. S2). At both depths (mixed layer and upper mesopelagic), there was a higher proportion of *Metazoa* affiliated sequences in SK10 and SS100, except at ICE, while a higher proportion of eukaryotic phytoplankton sequences was observed in SS0.22 and SS10 in the mixed layer (Table S1).

Hydrographic settings and community structure overview

The two less productive stations were located on the Antarctic continental ice-edge (ICE) and in a high-nutrients-low-chlorophyll (HNLC) zone (P2), whereas the two more

productive stations were located in a naturally iron-fertilized zone along South Georgia continental margin (P3) and in an upwelling zone at the frontal system of polar front zone and the Antarctic zone (UP) (Fig. 1). P3 and UP were in close proximity with each other and showed higher chlorophyll *a* concentrations (mean 1.90 and 1.23 $\mu\text{g L}^{-1}$ in the mixed layer, respectively), while ICE and P2 were further apart and had lower surface chlorophyll *a* concentrations (0.37 and 0.40 $\mu\text{g L}^{-1}$, respectively). There was a sharp temperature decrease between the mixed layer depth and the upper mesopelagic at all stations except ICE, at which the surface temperature was low ($< -1^\circ\text{C}$) due to freshly melted ice (Fig. S1). At all stations, POC concentrations were higher in suspended particles (Table S2), and within the mixed layer depth compared to the upper mesopelagic (Belcher et al. 2016b).

The CCA analysis based on protist OTU composition (Fig. 2) revealed a clear separation between stations, as well as between mixed layer and upper mesopelagic samples when considering each station individually. A PERMANOVA analysis calculated for phototrophic, and heterotrophic protist communities (Table S3)

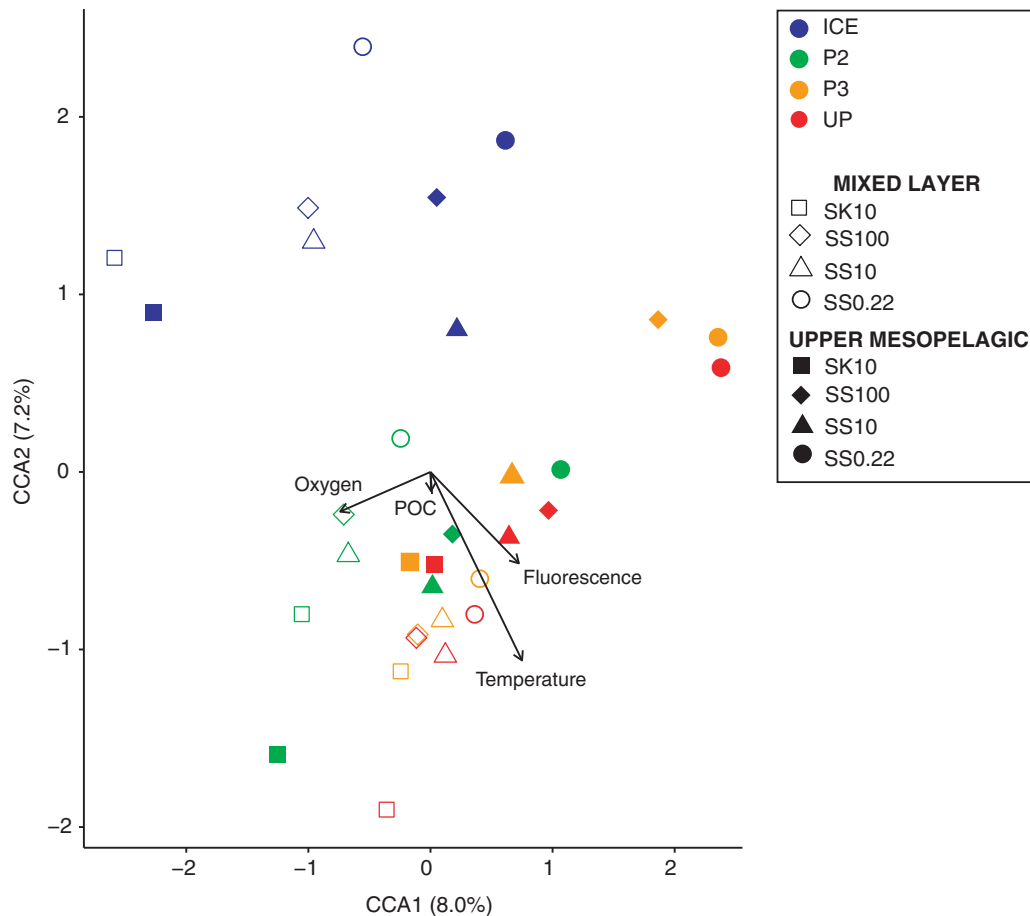


Fig. 2. CCA of OTU composition. The CCA was calculated on the total rarefied data set. The significance of environmental parameters (oxygen, fluorescence, POC concentrations, and temperature) was tested with a PERMANOVA ($p < 0.05$) (Table S3). Significant environmental parameters are displayed and the arrow length is proportional to the variability in community structure they explain. SS0.22, suspended particles 0.22–10 μm ; SS10, suspended particles 10–100 μm ; SS100, suspended particles $\geq 100 \mu\text{m}$; (SS100), SK10, sinking particles $\geq 10 \mu\text{m}$.

revealed that every environmental parameter tested (i.e., oxygen, fluorescence and POC concentrations, and temperature) as well as the particle fraction (SK10, SS100, SS10, and SS0.22) were significant predictors of OTU composition ($p < 0.05$), the latter explaining ~18% of observed variability. Similar to prokaryotic communities collected in identical particle fractions (Duret et al. 2018), protist communities collected at ICE were the most dissimilar compared to those collected at the other stations (P2, P3, and UP) (average Bray Curtis distance of 70.3% vs. 56.3%, respectively; Fig. 3). This is likely due to unique conditions present at ICE, located on the Antarctic continental ice edge (Fig. 1 and Fig. S1), compared to the other stations that were not influenced by melting-ice runoff (Atkinson et al. 2001). These conditions include negative temperatures (Chen and Laws 2017) and high concentrations of macro- (Garrison et al. 2005) and micronutrients release, such as iron and vitamin B₁₂ (Sedwick and Ditullio 1997; Taylor and Sullivan 2008). Although the addition of more ICE stations is needed to confirm their impacts, such differences in environmental conditions would have influenced eukaryotic phytoplankton and subsequently eukaryotic heterotrophic communities.

Eukaryotic phytoplankton components of the particle flux Surface eukaryotic phytoplankton communities

Overall, diatoms ($31.9 \pm 25.1\%$) and prymnesiophytes ($28.0 \pm 21.1\%$), and chlorophytes at ICE ($19.3 \pm 13.2\%$), dominated the phytoplankton communities in all particle fractions (i.e., SK10, SS100, SS10, and SS0.22) in the mixed layer

at every station (Fig. 4A). Assuming that phytoplankton sequences detected in the upper mesopelagic primarily originated from sinking particles in the mixed layer, the focus for eukaryotic phytoplankton communities was placed on sinking particles (SK10) in the mixed layer for subsequent comparison with sinking and suspended particles in the upper mesopelagic—in order to explore how phytoplankton components evolve with particle dynamics upon sinking. Expectedly, eukaryotic phytoplankton communities ($\geq 10 \mu\text{m}$) collected in the mixed layer differed largely between stations (Fig. 4A and Fig. S3), likely reflecting the different productivity regimes (Fig. 1). The less productive, iron-depleted HNLC station P2 was largely dominated by the prymnesiophyte *Phaeocystis*, representing 83.3% of eukaryotic phytoplankton sequences of SK10 in the mixed layer, which is consistent with literature. *Phaeocystis antarctica* is one of the most prevalent phytoplankton genera in the Southern Ocean, which has been reported within sea-ice (Brown and Bowman 2001) and to form large blooms in deeply mixed waters of the Ross Sea during the Austral summer (Arrigo 1999; Zoccarato et al. 2016).

Diatom sequences represented only 15.6% of SK10 eukaryotic phytoplankton sequences in the mixed layer at P2, but they averaged at $69.6 \pm 9.7\%$ in ICE, and the more productive stations P3 and UP. The polar centric diatom families *Coscinodiscophyceae* and *Mediophyceae* represented most of these sequences, the former being more abundant at ICE (34.0% vs. 12.0% at the other stations) and the latter at P2,

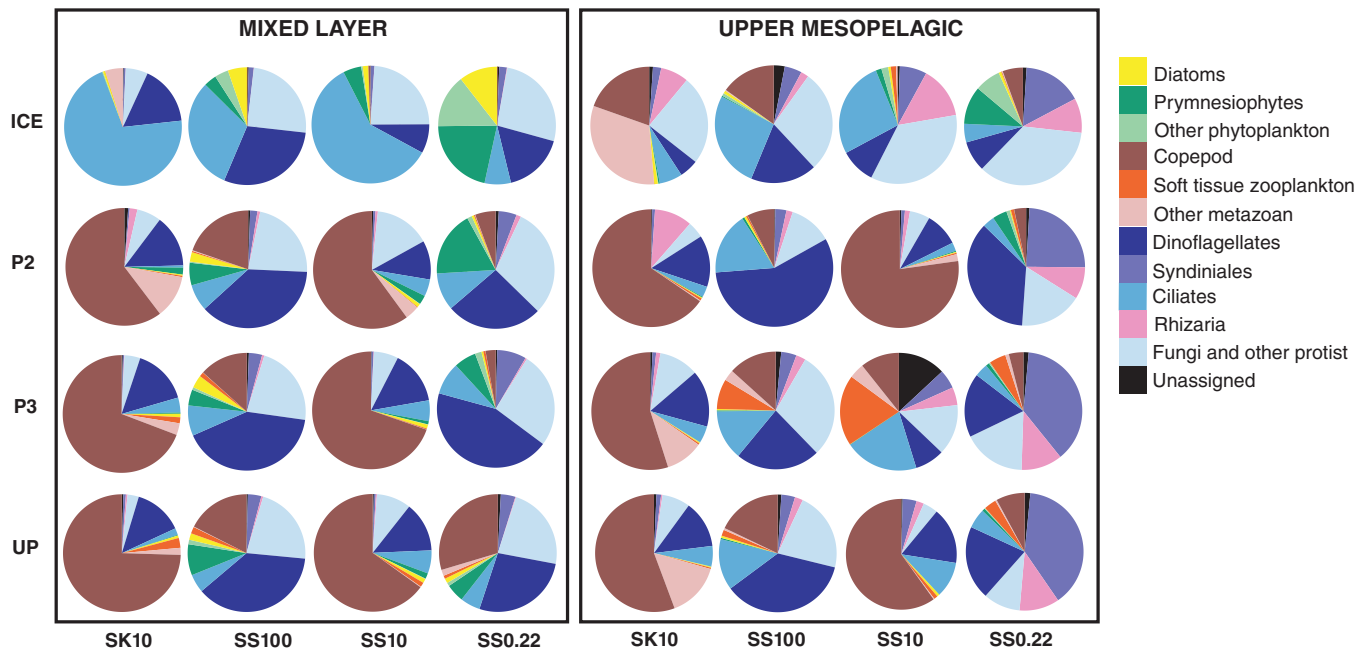


Fig. 3. Total eukaryotic community composition. Pie charts were constructed with the relative abundance of selected taxa in the total rarefied data set. Sequences were subcategorized into metazoan (copepod, soft-tissue animal, and other), phytoplankton (diatom, prymnesiophyte, and other), other protists and fungi (dinoflagellates, *Syndiniales*, ciliates, *Rhizaria*, and other), and unassigned sequences. SS0.22, suspended particles 0.22–10 μm ; SS10, suspended particles 10–100 μm ; SS100, suspended particles $\geq 100 \mu\text{m}$; (SS100), SK10, sinking particles $\geq 10 \mu\text{m}$.

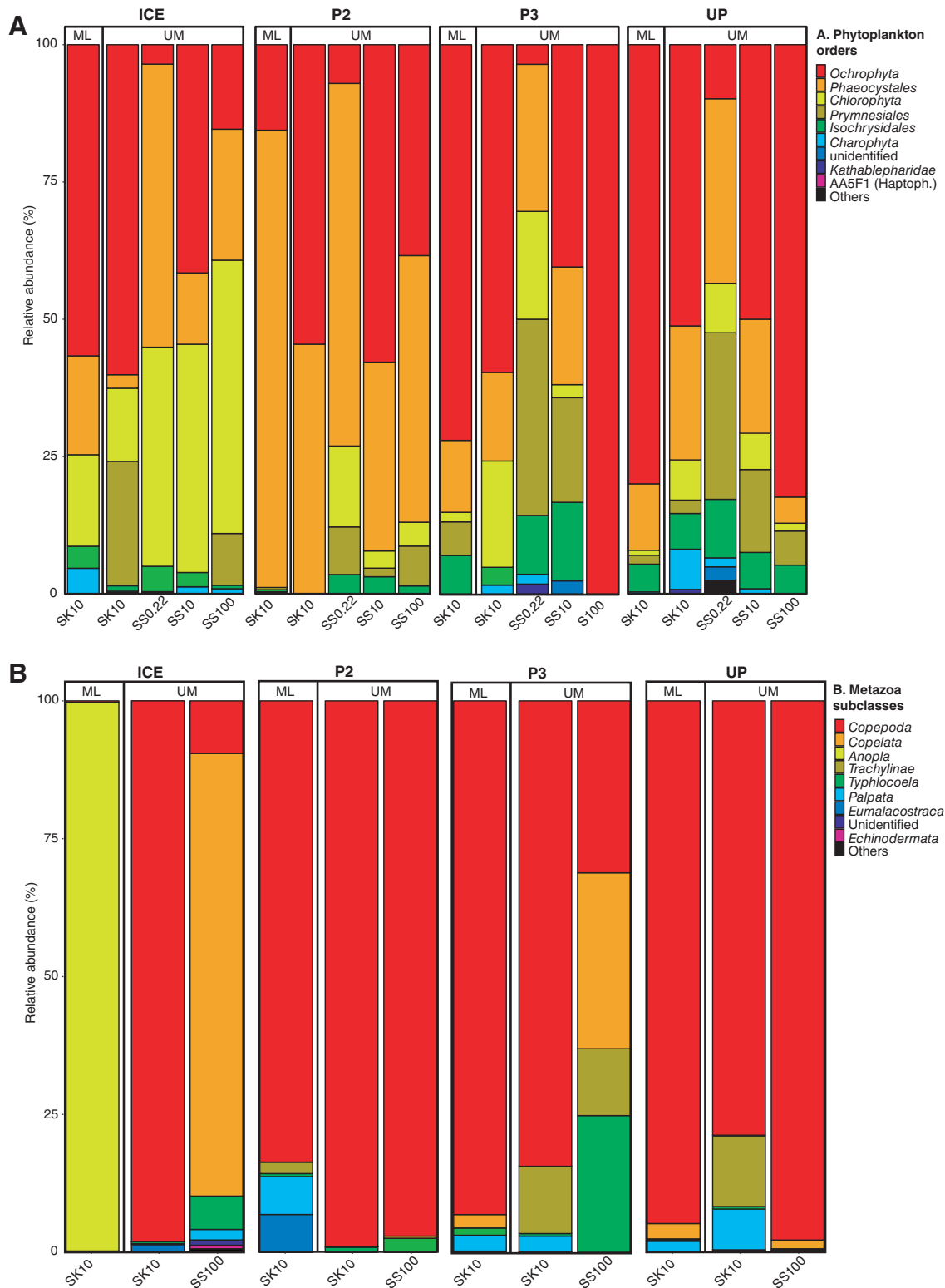


Fig. 4. Taxonomic composition of phytoplankton and metazoans. **(A)** Relative abundance of the nine most abundant phytoplankton orders, and **(B)** relative abundance of the nine most abundant metazoan subclasses. Presented data were normalized to the considered taxonomic group (i.e., phytoplankton and metazoans). SS0.22, suspended particles 0.22–10 μm ; SS10, suspended particles 10–100 μm ; SS100, suspended particles ≥ 100 μm ; (SS100), SK10, sinking particles ≥ 10 μm ; ML, mixed layer; UM, upper mesopelagic; Haptoph., Haptophyte.

P3, and UP (11.9% vs. 42.5%, respectively). *Actinocyclus* and *Corethron* were the dominant sinking diatoms at ICE (34.0%). Conversely, *Chaetoceros* (13.8%) along with unidentified members of the *Mediophyceae* family (27.5%) were the dominant sinking species at P3 and UP. *Coscinodiscophyceae* and *Mediophyceae* diatoms have consistently been reported in polar waters (Poulton et al. 2010; Rodríguez-Marconi et al. 2015; Zoccarato et al. 2016). In particular, *Actinocyclus* (*Coscinodiscophyceae*) and *Chaetoceros* (*Mediophyceae*) have frequently been detected in polar waters naturally enriched in iron (Georges et al. 2014; Rembauville et al. 2016). This agrees with the environmental conditions present at each respective station. ICE, P3, and UP benefit from various iron inputs, unlike P2 that is located in a HNLC region (Fig. 1). While eukaryotic phytoplankton communities at ICE can use high concentrations of iron originating from melted sea-ice (Sedwick and Ditullio 1997; Taylor and Sullivan 2008), P3 and UP benefit from nutrient-rich upwelled waters at the South Georgia continental margin (Atkinson et al. 2001).

Comparison with sinking eukaryotic phytoplankton in the mesopelagic

Eukaryotic phytoplankton sequences in SK10 communities at the two depths exhibited differences in terms of their structure and diversity (Figs. 4A and 5, and Fig. S3). *Mediophyceae* diatoms, mostly represented by *Chaetoceros*, accounted for

41.5 ± 13.0% of eukaryotic phytoplankton sequences collected in the SK10 fraction in the upper mesopelagic at every station, while *Coscinodiscophyceae* were mostly absent, except at P2 where they represented 13.0% of eukaryotic phytoplankton sequences. As *Actinocyclus* (*Coscinodiscophyceae*) was present in higher relative abundance in SK10 samples in the mixed layer than in the upper mesopelagic at ICE, P3, and UP, and similar relative abundance at P2, our data imply that few *Actinocyclus* sank out from the mixed layer. Using a similar logic, our data imply that it was mostly *Chaetoceros* that were exported to the upper mesopelagic. This apparent differential export is in agreement with literature on carbon export owing to different diatom groups (Leblanc et al. 2018). The fast-growing *Chaetoceros* has been correlated with high carbon export to depth, while the opposite is true for *Actinocyclus* that has been reported to be negatively correlated with POC export (Tréguer et al. 2018). Although *Actinocyclus* has a large biovolume, unlike *Chaetoceros*, it does not form chains (e.g., Poulton et al. 2010), which thereby lead to a reduction of its sinking velocity (Bannon and Campbell 2017). Additionally, higher grazing pressures on single *Actinocyclus* cells compared to chains of *Chaetoceros* (Hoffmann et al. 2008) could also lead to the difference observed in their carbon export potential. Larger cells are indeed more easily grazed (Smetacek et al. 2002) and chain-forming represents an effective way of protection against grazers (Pahlow et al. 1997).

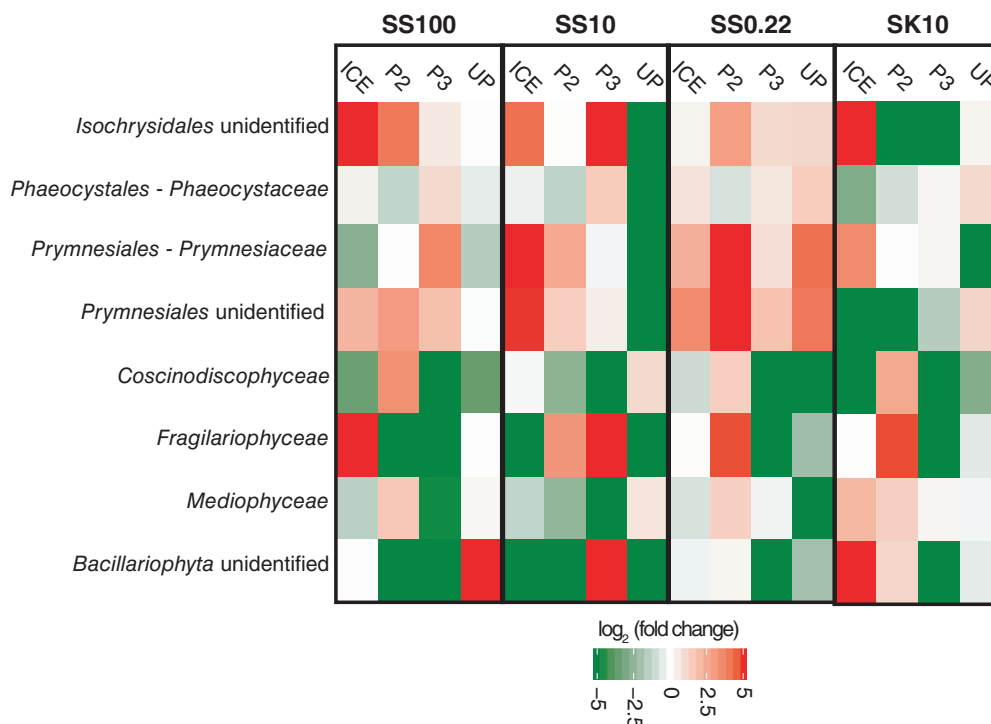


Fig. 5. Enrichment of phytoplankton taxonomic families in sinking and suspended particles. Enrichments were calculated using Eq. 1 on the phytoplankton normalized data set. Negative values indicate an enrichment within sinking particles in the mixed layer and positive values indicate an enrichment within the compared sample in the upper mesopelagic. SS0.22, suspended particles 0.22–10 μm ; SS10, suspended particles 10–100 μm ; SS100, suspended particles $\geq 100 \mu\text{m}$; (SS100), SK10, sinking particles $\geq 10 \mu\text{m}$.

By increasing death rates of *Actinocyclus*, micrograzers and copepods would increase their retention and remineralization in the mixed layer and thus limit their export to the upper mesopelagic. This potentially explains why *Actinocyclus* did not contribute as much as *Chaetoceros* to carbon export to the upper mesopelagic. Furthermore, the presence of *Chaetoceros* sequences in SK10 fractions agrees well with the observations of chain-forming centric diatoms via light microscopy in sinking particles collected in the upper mesopelagic during the same cruise (Belcher et al. 2016b).

Aggregates and fecal pellets that are ballasted by biogenic minerals, such as opals produced by diatoms, sink significantly faster than those that are not (Klaas and Archer 2002; Ploug et al. 2008). As they sink faster, particles are less susceptible to the increased remineralization processes in the upper mesopelagic (Martin et al. 1987) and can therefore sink deeper, leading to more efficient long-term carbon sequestration (Kwon et al. 2009). This is one of the reasons why diatoms are assumed to be more efficient carbon transporter to the deep ocean (Armstrong et al. 2002; Jin. et al. 2006) as opposed to non-ballasted phytoplankton taxa such as *Phaeocystis*.

At P2, where prymnesiophytes were most dominant in the mixed layer, fewer sequences belonging to *Phaeocystis* were retrieved in SK10 in the upper mesopelagic compared to the mixed layer (45.5%). This implies that despite its abundance in the mixed layer, this taxon was not as efficient as diatoms for carbon export to the deep ocean. Instead, *Phaeocystis* was observed primarily in the upper mesopelagic small-suspended fraction (SS0.22), suggesting that although they contributed to the POM flux out of the euphotic zone to some extent, *Phaeocystis*-enriched particles were subject to higher remineralization and thus unlikely to sink to depths below the upper mesopelagic. *Phaeocystis* has previously been reported as a key component of POC export in polar waters (DiTullio et al. 2000), as they have the

ability to form aggregates that sink rapidly out of the mixed layer (Arrigo 1999). However, during our study this eukaryotic phytoplankton appeared to contribute little to carbon transfer efficiency, especially compared to its diatom counterparts as observed elsewhere in Antarctic waters (Lin et al. 2017). The rapid export of *Phaeocystis* out of the euphotic zone is generally related to their enhanced production of transparent exopolymer polysaccharides (TEP; Passow et al. 2001). TEP production in *Phaeocystis* tends to increase when colonies start to die (Hong et al. 1997). However, TEP-enriched particles have a reduced density that, if they are not ballasted enough (Mari et al. 2017), show a reduced sinking velocity or can even be buoyant (Eberlein et al. 1985).

Although some cyanobacteria sequences were also present in the same samples according to parallel 16S rRNA gene amplicon sequencing data set, we surmise that their contribution to the phytoplankton component of the BCP would be relatively small. Cyanobacteria sequences were only detected in low numbers in 19 out of 32 samples (Table S4 and Fig. S4A), and appeared more enriched in the upper mesopelagic, especially in SK10 (Table S4B). Their apparently low abundance is consistent with previous report of their scarcity in the Scotia Sea (Jacques and Panouse 1991), and generally in polar waters in favor of diatoms and prymnesiophytes (Ishikawa et al. 2002; Doolittle et al. 2008; Yang et al. 2012). Therefore, eukaryotic phytoplankton appeared to be the dominant phytoplankton driver of the BCP in the Scotia Sea.

At stations P2, P3, and UP, $87.1 \pm 3.4\%$ of eukaryotic phytoplankton sequences collected in SK10 in the upper mesopelagic were affiliated with OTUs shared with SK10 in the mixed layer (representing $23.1 \pm 2.0\%$ of OTUs in the upper mesopelagic), while at ICE only 32.0% of sequences belonged to OTUs common between SK10 at both depths (12.8% of OTUs) (Table 1). This suggests that, at least in P2, P3, and UP, phytoplankton diversity observed in sinking particles in the upper mesopelagic

Table 1. Percentages of OTUs and affiliated sequences shared between particle fractions. The proportions of phytoplankton and meta-zoan shared OTUs were calculated on the rarefied data set.

			ICE		P2		P3		UP	
			OTU	Seq	OTU	Seq	OTU	Seq	OTU	Seq
Phytoplankton	SK10 ML with	SK10 UM	12.8	32.0	22.6	89.6	20.9	82.3	25.8	89.4
		SS100 UM	23.7	80.8	25.0	82.6	10.5	100.0	25.4	72.9
	SS ML with	SS10 UM	25.5	76.9	29.4	82.8	19.5	92.9	37.5	88.7
		SS0.22 UM	17.1	72.9	16.0	77.9	15.4	71.4	19.5	73.0
		SS100 UM		57.6		12.9		0.3		17.1
		SS10 UM	29.0	14.8	35.7	3.3	21.3	2.1	26.9	5.3
Metazoan	SK10 ML with	SS0.22 UM		42.0		4.2		0.7		1.5
		SK10 UM	4.5	90.7	20.4	99.4	31.0	72.8	22.3	87.0
		SS100 UM	10.0	2.9	11.0	96.9	5.8	80.2	23.7	99.5

SS0.22, suspended particles 0.22–10 μm ; SS10, suspended particles 10–100 μm ; SS100, suspended particles $\geq 100 \mu\text{m}$; (SS100), SK10, sinking particles $\geq 10 \mu\text{m}$; ML, mixed layer; UM, upper mesopelagic; OTU, % OTUs shared; Seq, % affiliated sequences.

likely originated from the mixed layer. Furthermore, a similar proportion of SK10 sequences was shared with suspended particle size fractions at the upper mesopelagic from all stations ($91.9 \pm 5.2\%$ representing $11.8 \pm 0.8\%$ of OTUs). This therefore suggests strong interchanges between sinking and suspended particles in the upper mesopelagic, the latter likely originating from particles sinking out of the mixed layer. Contributors to the remaining unique OTUs may come from: (1) the export of small sinking particles from the surface ($< 10 \mu\text{m}$) (Dall'Olmo and Mork 2014) that would have not been sampled here, (2) the presence of low-light adapted phytoplankton in the upper mesopelagic (Jacques 1983), and/or (3) the lateral export of sinking particles from adjacent mesopelagic water masses.

Influences on suspended particles in the upper mesopelagic

In the upper mesopelagic, suspended particles 10–100 μm (SS10) and $> 100 \mu\text{m}$ (SS100) were largely dominated by prymnesiophytes ($32.4 \pm 18.9\%$), mostly represented by *Phaeocystis*, and by diatoms ($55.6 \pm 24.7\%$) mainly belonging to *Proboscia* (*Coscinodiscophyceae*) at P3, *Thalassionema* (*Fragilariophyceae*) at UP, and unidentified members of *Mediophyceae* at ICE and P2 (Fig 4A and Fig. S3). Regardless of the station, *Phaeocystis* dominated suspended particles 0.22–10 μm (SS0.22) ($44.5 \pm 15.4\%$). Furthermore, every suspended particle size fraction in the upper mesopelagic at ICE contained high proportions of chlorophyte sequences ($36.8 \pm 14.0\%$). Prymnesiophytes and unidentified chlorophytes were particularly enriched in each suspended particle size fractions in the upper mesopelagic compared to SK10 in the mixed layer (Fig. 5 and Fig. S3). Notably, the chlorophyte *Prasinophyceae* clade VIII (Viprey et al. 2008) was only present in SS0.22 samples at ICE.

Most sequences retrieved from all suspended particle fractions in the upper mesopelagic were common with those in SK10 in the mixed layer at all stations ($81.1 \pm 8.6\%$, representing $22.0 \pm 6.9\%$ of OTUs), thus again reaffirming the fact that particles sinking from mixed layer are more likely the source for suspended particles in the upper mesopelagic. Suspended particles in the mesopelagic can originate (1) from the disaggregation of sinking particles, through the action of biotic and abiotic processes (Lam and Marchal 2015), (2) from *in situ* chemolithoautotrophic primary production in the mesopelagic (Aristegui et al. 2009), and also (3) from vertical mixing or lateral transport, which lead to the introduction of suspended material from adjacent water masses (Baltar et al. 2009). As only photosynthetic primary producers are considered in this section and owing to the high proportion of shared sequences between suspended particles in the upper mesopelagic and sinking particles at both depths, the diversity observed in suspended particles in the upper mesopelagic would therefore originate from the surface mixed layer, that is, likely from sinking particles disaggregation and/or vertical and lateral mixing.

Furthermore, the enrichment of prymnesiophytes, and particularly of *Phaeocystis*, in every suspended particle size fractions, coupled with the enrichment of diatoms in sinking particles in the upper mesopelagic, supports the differential particle dynamics observed existing between prymnesiophyte-enriched and diatom-enriched particles (Figs. 4A and 5). On the one hand, prymnesiophyte-enriched particles sinking from the mixed layer were more likely to break down into suspended particles in the upper mesopelagic. On the other hand, diatom-enriched particles were more likely to sink faster and deeper into the ocean, owing to their larger cell sizes and mineral ballasting. This is in agreement with the observed influence of phytoplankton community structure on carbon export (Giering et al. 2017). At ICE, the higher proportion of OTUs shared between suspended particles in the mixed layer and those in the upper mesopelagic compared to other stations suggests a bigger influence of vertical mixing that led to the intrusion of surface suspended particles deeper in the water column. This is consistent with the chlorophyll *a* profile observed at the ICE station (Fig. S1). However, this is not in agreement with the water column stabilization effect (Petrou et al. 2016) generally expected from Antarctic continental ICED melted runoffs (Atkinson et al. 2001) and the mixing observed at ICE was possibly caused by regional hydrographic effects that remained to be determined.

Metazoan components of the particle flux

For metazoans, our focus was placed on SK10 and SS100 where most of the larger fragments of organisms and whole organisms ($> 100 \mu\text{m}$) would have been recovered, and thus be most informative regarding their influences on sinking vs. suspended particles. Metazoan sequences were most abundant in these fractions compared to SS10 (except at ICE) and SS0.22 (Table S1). Metazoan sequences recovered in SS10 and SS0.22 likely corresponded to small fragments of organisms and/or fecal pellets.

The diversity of sequences collected in SK10 in the mixed layer was similar to that of the upper mesopelagic, as $87.5 \pm 9.6\%$ of metazoan sequences and $19.6 \pm 9.6\%$ of OTUs were shared between the two particle pools (Table 1). Nonetheless, the compositions of metazoan sequences in SK10 at the two depths were different (Fig. 4B and Fig. S5). Except in the mixed layer at ICE, SK10 samples were dominated by copepod sequences ($90.4 \pm 5.1\%$), which were mostly affiliated with *Calanoida* ($67.6 \pm 6.7\%$) and *Cyclopoida* ($20.9 \pm 6.0\%$). This agrees with results from Belcher et al. (2016b) that attributed more than half of sinking POC flux at this station to calanoid fecal pellets. Due to their relatively fast sinking, POC export dominated by mesozooplankton fecal pellets generally leads to limited connectivity between sinking and suspended particle pools in the mesopelagic. Fecal pellets are indeed more resistant to remineralization compared to phytoplankton-dominated particles and conferred low microbial respiration rates (Belcher et al. 2016 and 2016b), as they have higher densities and are surrounded by a protective membrane

(Abramson et al. 2010). Beside their role in repackaging surface primary production into fecal pellets (Turner 2015), mesozooplankton are also responsible for the breakage of sinking particles (e.g., sloppy feeding, Steinberg and Landry, 2017, and microbial gardening, Mayor et al. 2014) and contribute to the creation of smaller suspended particles, thereby connecting the two particle pools together (Lam and Marchal 2015).

In the upper mesopelagic, sequences retrieved from SS100 and SK10 at ICE and P3 showed slightly enhanced differences compared to those from P2 and UP (Table 1). While SK10 at ICE and P3 were dominated by copepod sequences (> 80.0%), SS100 was dominated by sequences that belonged to the more soft-bodied organisms, including the tunicate family *Oikopleuridae* at ICE, while at P3 *Oikopleuridae*, the ctenophore class *Typhlocoela* and cnidarian class *Trachylinae*. Such distinction suggests different roles played by mesozooplankton taxa in sinking and suspended particle pools within the upper-mesopelagic ocean.

The main limitations of these results are that (1) living copepods could have swum towards the bottom of the MSC to feed on sinking particles within the time frame of particle settling (2 hr), which would subsequently have reduced their detection in suspended particles (i.e., in the upper part of the MSC); and that (2) the exact source of detected DNA is difficult to determine. That is, the DNA collected could indicate the presence of the organisms (e.g., copepods) themselves while alive, or merely fragments of shredded or dead body parts (e.g., antennas, broken shells), residual genetic materials present in fecal pellets, or allochthonous materials advected into the sampled site and depth. Nonetheless, these results indicated that while copepods were more influential on sinking particles, either with their fecal pellets or by their feeding behaviors, the soft-bodied *Oikopleuridae*, *Typhlocoela*, and *Trachylinae* were more important for suspended particles, especially in the more productive stations. Suspended particles could represent an organic substrate for these animals, as it was suggested in the central North Pacific (Gloeckler et al. 2017). Alternatively, their soft-tissue structures and/or secretions could actually be a major component of suspended particles themselves acting as a binder for smaller particles and DOM, similar to empty larvacean houses, without ever reaching densities high enough to sink as is sometimes observed (Alldredge 1976; Simon et al. 2002; Wilson et al. 2008).

The use of 18S rRNA gene amplicon sequencing to investigate the contribution of metazoans to suspended and sinking particles represents a useful complement to classic microscopic analyses, which usually focuses only on large, sinking particles, and is limited by recognizable morphologies of body parts, often missing the smaller and amorphous fragments. Our amplicon sequencing approach shares the same metabarcoding principle as the increasingly applied environment DNA (eDNA) approach (Thomsen et al. 2012; Andruszkiewicz et al. 2017; Flaviani et al.

2017; Djurhuus et al. 2018). They also share the same limitations by the degree of quantitative information the data could convey due PCR biases and different amounts of DNA or gene copies present in the organisms (part or whole) concerned.

Heterotrophic protists and fungi associated with particles Community connectivity with depth and method limitations

Given their high numerical abundances and various trophic modes (Sherr and Sherr 2002; Worden et al. 2015; Stoecker et al. 2017), such as in polar environments (Korb et al. 2012; Caron et al. 2016), heterotrophic protists are key players in the remineralization and cycling of organic matter. The abundances of specific groups of heterotrophic protists varied among sampled stations and depths, which were likely influenced by the inherent environmental conditions (Fig. 2) and reflected a geographic niche specialization amongst heterotrophic protists as has been observed in various oceanic environments (Williams et al. 2018). Nonetheless, OTU composition was mainly driven by the particle fraction which explained 18.4% of OTU variability ($p < 0.05$) (Table S3). Heterotrophic protist communities in the mixed layer were on average $43.2 \pm 15.1\%$ dissimilar compared to $58.5 \pm 14.9\%$ in the upper mesopelagic (Table S5). Every particle fraction in the upper mesopelagic was on average $66.6 \pm 13.6\%$ dissimilar compared to SK10 in the mixed layer. This agrees with the literature showing that heterotrophic protist assemblages from the surface differ from those from the mesopelagic and deeper (López-García et al. 2001; Edgcomb et al. 2011; Orsi et al. 2012; Pernice et al. 2014, 2016; Duret et al. 2015; Zoccarato et al. 2016). However, heterotrophic protist communities in the mesopelagic ocean and below remain largely unknown (Edgcomb 2016; Caron 2017), especially in the Southern Ocean, despite the fact that most POC flux attenuation and thus remineralization typically occurs within the mesopelagic (Martin et al. 1987). In order to get an insight into the roles of heterotrophic protists in remineralization processes and particle dynamics processes where they are most active, the following section focuses on differences between particle fractions collected in the upper mesopelagic.

In the meso- and bathypelagic, ciliates are scarce (Aristegui et al. 2009; Morgan-Smith et al. 2013; Bochdansky et al. 2017) compared to heterotrophic nanoflagellates (e.g., Tanaka and Rassoulzadegan 2002; Gowing et al. 2003; Pernice et al. 2014; Dolan et al. 2017). Despite nanoflagellates biomass sometimes exceeding that of ciliates (Safi et al. 2012), the latter usually dominate the relative abundance of 18S rRNA gene amplicon sequencing data sets (e.g., Countway et al. 2005; Duret et al. 2015; Pernice et al. 2016) owing to high numbers of SSU rRNA gene copies and DNA content (Zhu et al. 2005; Gong et al. 2013). The accurate quantitative detection of other alveolates, such as dinoflagellates (Godhe et al. 2008), and rhizarians, that is, radiolarians (Suzuki and Aita 2011) and colpodarians (Biard et al. 2017), presents similar limitations owing to their high numbers of gene copies.

Alveolata were the most abundant taxa among all samples in our data set (Fig. 3), representing $84.7 \pm 13.0\%$ of heterotrophic sequences. While *Dinoflagellata* sequences were relatively abundant in all particle fractions ($37.5 \pm 18.3\%$), the parasitic *Protalveolata* sequences were most abundant in SS0.22 ($34.0 \pm 9.9\%$ vs. $5.7 \pm 2.6\%$ in other particle fractions), and *Ciliophora* sequences were most abundant in SS100, SS10 and SK10 ($21.5 \pm 8.7\%$ vs. $5.0 \pm 1.5\%$ in SS0.22) (Fig. S6A and S6B, Table S1). Although ciliates (Caron et al. 1982; Silver et al. 1998; Gowing et al. 2001) and radiolarians (Lampitt

et al. 2009; Biard et al. 2016) have been reported associated with particles in the mesopelagic, our data set does not accurately inform on their true abundance compared to smaller heterotrophs that are equally important in top-down control of phytoplankton and bacterial communities in cold waters (Garzio et al. 2013). Relative abundances presented below were normalized within category (i.e., dinoflagellates, choanoflagellates, *Syndiniales*, ciliates, rhizarians, and fungi) (Fig. 6) in order to better visualize differences between less represented taxa.

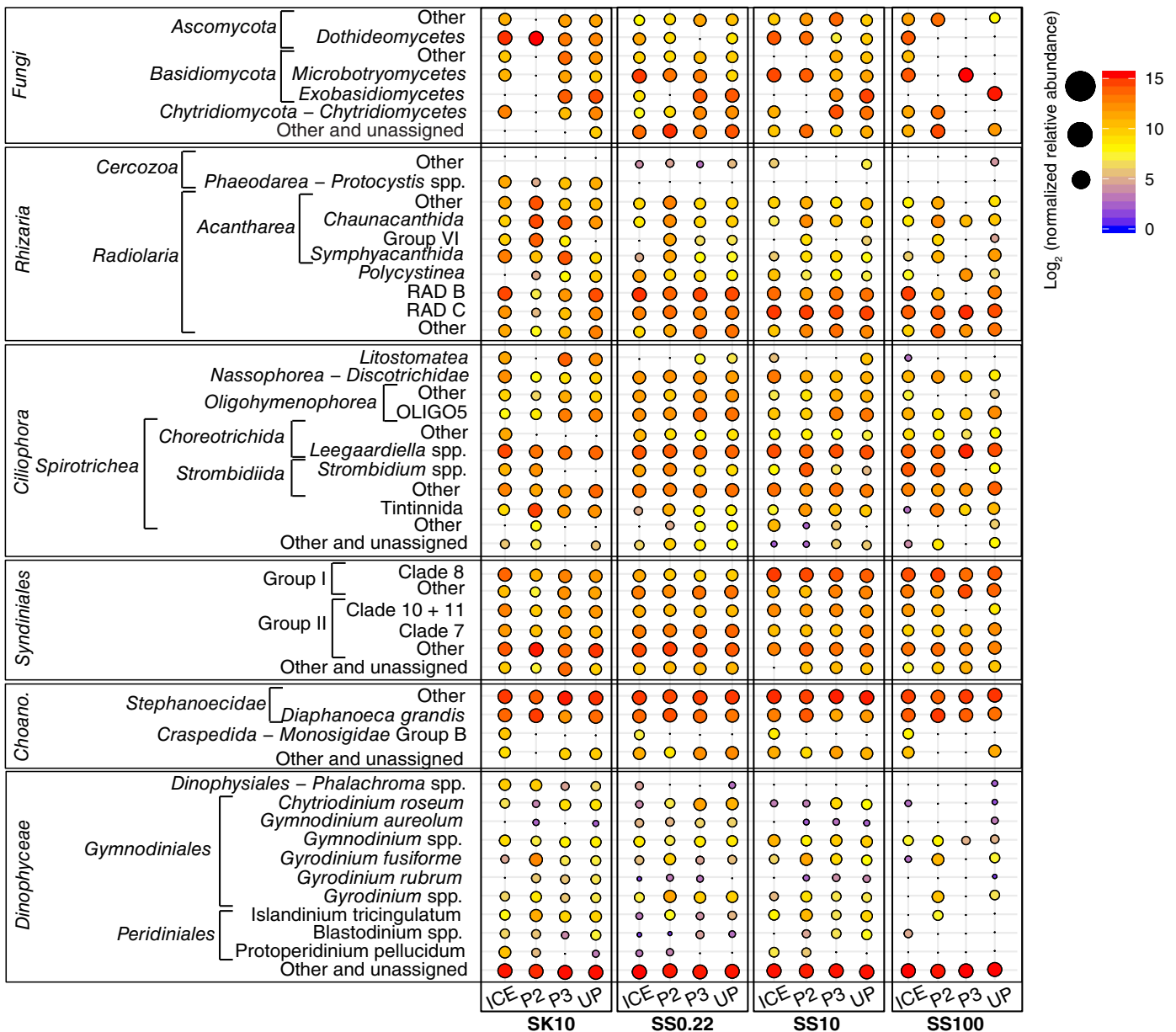


Fig. 6. Heterotrophic protists and fungi communities in sinking and suspended particles in the upper mesopelagic. Presented data were normalized to the considered taxonomic category (i.e., dinoflagellates, choanoflagellates, *Syndiniales*, ciliates, rhizarians, and fungi), and transformed using the formula $\log_2(x) + 1$ when $x > 0$ and where x is the relative abundance normalized within the taxonomic category considered. SS0.22, suspended particles 0.22–10 μm ; SS10, suspended particles 10–100 μm ; SS100, suspended particles $\geq 100 \mu\text{m}$; (SS100), SK10, sinking particles $\geq 10 \mu\text{m}$; Choano., Choanoflagellata.

Flagellates

While certain dinoflagellates taxonomic groups were enriched in specific particle fractions, differences between stations were important. *Gymnodiniales* sequences were overall least abundant at ICE ($2.19 \pm 1.58\%$) than at P2 ($9.98 \pm 3.14\%$), and were less represented in SS100 than other particle fractions. Different *Gyrodinium* species (*Gymnodiniaceae*) were enriched in specific particle fractions, with *Gyrodinium fusiforme* most abundant in SS10 and SK10 at P2, *Gyrodinium rubrum* in SK10, and unidentified *Gyrodinium* spp. in SS0.22. *Gyrodinium* cells (10–100 μm) are able to feed on phytoplankton cells much bigger than themselves, such as diatoms (Sherr and Sherr 2007). They have thus been negatively correlated with POC export in the Southern Ocean owing to their grazing activities (Cassar et al. 2015; Lin et al. 2017). *Gymnodinium* spp. was most enriched in SS10, and *Gymnodinium aureolum* was most enriched in SS0.22. These unarmored dinoflagellates can either be autotrophic, such as *G. aureolum*, forming blooms (Garrison et al. 2005; Jeong et al. 2010), or ectoparasites (Gómez et al. 2009). The recovery of *G. aureolum* in SS0.22 could correspond to cells living freely in the water column, while those recovered in SS10 could correspond to parasitic species. The crustacean eggs ectoparasite *Chytriodinium roseum* (Gómez et al. 2009) was however most abundant in SS0.22. The copepod parasite genera *Blastodinium* spp. (Skovgaard et al. 2012) was well represented in SK10 and SS100, and likely correspond to dinoflagellates hosted by copepods recovered in these larger size fractions ($\geq 100 \mu\text{m}$).

Peridinales sequences were most abundant in SK10 and SS100. Two cold water ubiquitous predatory motile flagellates *Islandinium tricingulatum* and *Proto-peridinium pellucidum* (Okolodkov 1999; Head et al. 2001) were most abundant in SK10. Furthermore, the ubiquitous predatory *Phalacrochroma* spp. (*Dinophysiales* - *Oxyphysiaceae*) (Jensen and Daugbjerg 2009) was most abundant in SK10 at all stations.

Choanoflagellates (*Holozoa*) sequences were mostly represented by the taxonomic family *Stephanoecidae* (*Acanthoecida*), belonging mostly to *Diaphanoeca grandis* in SS100 and by group H in SK10 and SS10. *Stephanoecidae* choanoflagellates are ubiquitous bacterivorous predators (Marchant 1985) measuring between 3 and 10 μm (Kirchman 2008) that are regularly detected in polar waters (Smith et al. 2011; Georges et al. 2014). Their detection in larger particle size fractions suggests an active colonization by these nanoflagellates of sinking and suspended particles $\geq 100 \mu\text{m}$. Alternatively, their detection could be indicative of colony formation (Thomsen et al. 1991). Sequences from the choanoflagellates family *Monosigidae* group B (*Craspedida*) were only detected at ICE, mostly in SK10.

Parasitic *Syndiniales* sequences are commonly detected in 18S rRNA gene sequencing in high abundances (e.g., Sauvadet et al. 2010; de Vargas et al. 2015; Cleary and Durbin 2016; Gutierrez-Rodriguez et al. 2019). They affect a wide variety of hosts, ranging from diatoms (Berdjeb et al. 2018), tintinnids

(Harada et al. 2007), and radiolarians (Dolven et al. 2007) to copepods (Skovgaard et al. 2005). Sequences belonging to the parasitic *Syndiniales* showed strong enrichment patterns. SS10 was most enriched in group I clade 8, SS100 in group II clade 10 + 11 as well as group I clade 8. SS0.22 was most enriched in group II clade 10 + 11 and clade 7. The latter clade has been mostly recovered in aphotic layers and is hypothesized to be affecting radiolarians in the mesopelagic (Guillou et al. 2008). The detection of *Syndiniales* group II has been reported in the small fraction of Antarctic waters previously (López-García et al. 2001), and could correspond to the detection of dinospores (1–12 μm) dispersed in the water column (Guillou et al. 2008). Group I has been recovered from anoxic and suboxic samples more systematically than group II (Guillou et al. 2008), and their detection mostly in suspended particles $\geq 10 \mu\text{m}$ could indicate the presence reduced conditions in this particle pool. SK10 had a more diverse composition, which could indicate more transient conditions and/or the presence of a variety of hosts associated with sinking particles.

Although represented within each particle fractions, most predatory flagellate sequences were recovered in sinking particles. These predators likely feed on sinking particle-associated bacterial populations (Fenchel 1982a,b,c; Sherr and Sherr 2002) and phytoplanktonic cells within particles (Sherr and Sherr 2007). Their more important detection on sinking particles could reflect the presence of their preferred bacterial prey (e.g., Anderson et al. 2013). This in turns is in agreement with the differential bacterial communities associated with sinking and suspended particles collected during the same cruise (Duret et al. 2018). Additionally, their detection in sinking particles rather than in other large suspended particles might have been artificially created in the MSC by the creation of a chemical gradient as particle sank to the bottom of the sampler, which would have cause them to preferentially colonize these particles by chemotaxis (Fenchel 2001). It is nonetheless important to keep in mind that most dinoflagellates sequences could not be annotated at a high taxonomic resolution under PR² or Silva (representing $91.8 \pm 5.1\%$ of dinoflagellates sequences) and could correspond to predatory species.

Ciliates

Ciliate sequences did not present evident enrichment patterns in sinking or suspended particles $\geq 10 \mu\text{m}$, suggesting that their detection reflected their cell sizes (generally $> 40 \mu\text{m}$) and/or their attachment to both particle fractions $> 100 \mu\text{m}$. These predators likely act in the top-down controls of bacterial prey populations associated with suspended and sinking particles (Caron et al. 2012). Nonetheless, sequences affiliated with *Tintinnida* and *Litostomatea* at P2 were slightly more abundant in SK10 than other particle fractions, both of which have previously been detected in various mesopelagic sites (e.g., Grattepanche et al. 2016; Zoccarato et al. 2016; Dolan et al. 2017). Furthermore, sequences belonging to

OLIGO5 (*Oligohymenophorea*) and *Discotrichidae* (*Nassophorea*) were slightly more abundant in SS0.22 at most stations.

Most ciliate sequences were affiliated with *Choreotrichida* and *Strombidiida* (*Spirotrichea*) in every samples. These sequences were mainly represented by *Leegaardiella* sp. and *Strombidium* sp., respectively, the latter being mainly present at P2. Both genera include heterotrophic and mixotrophic species that have been reported to be important components of the ciliate communities in Arctic waters (Jiang et al. 2015). While *Leegaardiella* spp. are mainly reported to be heterotrophic, *Strombidium* spp. are mostly mixotrophs (Dziallas et al. 2012) that have the ability to sequester chloroplasts from their phytoplankton prey (i.e., kleptoplastidy) and can therefore participate in primary production when light conditions allow (Stoecker et al. 2017).

Rhizarian

Unsurprisingly, most *Rhizaria* sequences belonged to radiolarians. Radiolarians are globally abundant in the mesopelagic ocean, where they represent a large proportion of the planktonic biomass (Biard et al. 2016; Boltovskoy and Correa 2016). These mostly mixotrophic organisms (Caron et al. 2012; Decelle et al. 2012; Flynn et al. 2013; Stoecker et al. 2017) are key components to the transfer of organic matter to the deep ocean, owing to their large cell sizes (40–400 μm) (Suzuki and Aita 2011) and their mineral exoskeleton acting as ballast, and are therefore regularly detected in sediment traps (e.g., Boyd and Trull 2007; Lampitt et al. 2009; Biard et al. 2018; Gutierrez-Rodriguez et al. 2019). Radiolarian sequences exhibited strong enrichment patterns in specific particle fractions. On the one hand, silica bearing radiolarians sequences (Suzuki and Not 2015) were most enriched in suspended particles, with RAD C most enriched in suspended particles $\geq 10 \mu\text{m}$ and RAD B in SS0.22. On the other hand, strontium sulfate bearing acantharians (Decelle et al. 2013) were most abundant in SK10, represented by *Symphyacanthida* at P3 and ICE, *Chaunacanthida* at P2, P3, and group VI at P2. These sequences could correspond to acantharian cysts, generally measuring up to 1 mm, which have been reported to participate to organic carbon export to depth (Decelle et al. 2013). Furthermore, sequences belonging to the heterotrophic *Phaeodaria* group were mostly enriched in SK10 and represented by *Protocystis* sp. This is also consistent with studies conducted in other oceanic regions, where they play an important role in organic carbon export (Biard et al. 2018; Stukel et al. 2018).

The differential enrichment of radiolarians in suspended and sinking particles could reflect various efficiencies in carbon export from the mixed layer to the upper mesopelagic between groups, with acantharians being more efficient than RAD B and C. Additionally, these differences could correspond to differential life stages (e.g., cyst, vegetative cell, free-living cell) or physiological state (heterotrophy or autotrophy).

Fungi

Rather than presenting enrichment patterns among particle fractions, fungi sequences presented most differences between stations. The sporous *Microbotryomycetes* (*Basidiomycota* - *Pucciniomycotina*) and filamentous *Dothideomycetes* (*Ascomycota* - *Pezizomycotina*) were most enriched at ICE, while the sporous *Chytridiomycetes* (*Chytridiomycota* - *Chytridiomycotina*) and *Exobasidiomycetes* (*Basidiomycota* - *Ustilaginomycotina*) were most enriched at P3 and UP. *Basidiomycota*, *Ascomycota*, and *Chytridiomycota* have been reported previously in frozen Antarctic lakes (Gonçalves et al. 2012; Rojas-Jimenez et al. 2017). Marine fungi have been reported to play important roles in organic matter degradation in upwellings (off the coast of Chile; Gutiérrez et al. 2010, 2011) and in particles in coastal regions (Taylor and Cunliffe 2016) and in the bathypelagic (Bochdansky et al. 2017). It is however difficult to conclude regarding their role within particles collected at the different stations, as they could either be heterotrophic or parasitic (Grossart et al. 2019).

Conclusion

This study provides the first insights into eukaryotic contribution to suspended and sinking particle pools in the mixed layer and the upper mesopelagic of the Scotia Sea. Amplicon sequencing of the 18S rRNA gene served as a powerful diagnostic tool to identify the major eukaryotic phytoplankton present in sinking particles that most likely drives the BCP strength, and gave insights into the influence of metazoans, heterotrophic protists, and fungi on sinking and suspended particles in the upper mesopelagic. Notably, the chain-forming genus *Chaetoceros* dominated the eukaryotic phytoplankton component of sinking particles thereby suggesting that they facilitated carbon flux out of the mixed layer to the upper mesopelagic. Prymnesiophyte-enriched particles appeared to be more easily broken down into suspended particles in the upper mesopelagic, conferring lower transfer efficiency to the BCP. Copepods, either by their feeding behavior and/or the production of dense fecal pellets, were more influential on sinking particles than on suspended particles; while at some stations, soft-tissue organisms were found to primarily affect suspended particles. Heterotrophic protists and fungi communities in the upper mesopelagic resembled little to their mixed-layer counterparts. The distinct community structures observed in various particle fractions suggests different ecological conditions existing within suspended and sinking particles, such as chemical composition of organic matter and prey population availability. Nonetheless, investigations into predator-prey specificities, organic matter requirements, as well as quantification of these heterotrophic groups are required to further understand their effects on suspended and sinking particles, as well as to decipher their respective roles in the BCP. Results from this study further highlight the need to consider the interactions of eukaryotic communities with

both sinking and suspended particles, along with the respective prokaryotic communities, when evaluating the strengths and controls of the BCP.

References

- Abramson, L., C. Lee, Z. Liu, S. G. Wakeham, and J. Szlosek. 2010. Exchange between suspended and sinking particles in the northwest Mediterranean as inferred from the organic composition of in situ pump and sediment trap samples. *Limnol. Oceanogr.* **55**: 725–739. doi:10.4319/lo.2009.55.2.0725
- Allredge, A. L. 1976. Discarded appendicularian houses as sources of food, surface habitats, and particulate organic matter in planktonic environments. *Limnol. Oceanogr.* **21**: 14–24. doi:10.4319/lo.1976.21.1.0014
- Anderson, R., C. Wylezich, S. Glaubitz, M. Labrenz, and K. Jürgens. 2013. Impact of protist grazing on a key bacterial group for biogeochemical cycling in Baltic Sea pelagic oxic/anoxic interfaces. *Environ. Microbiol.* **15**: 1580–1594. doi:10.1111/1462-2920.12078
- Andruszkiewicz, E. A., H. A. Starks, F. P. Chavez, L. M. Sassoubre, B. A. Block, and A. B. Boehm. 2017. Bio-monitoring of marine vertebrates in Monterey Bay using eDNA metabarcoding. *PLoS One* **12**: 1–20. doi:10.1371/journal.pone.0176343
- Aristegui, J., J. M. Gasol, C. M. Duarte, and G. J. Herndl. 2009. Microbial oceanography of the dark ocean's pelagic realm. *Limnol. Oceanogr.* **54**: 1501–1529. doi:10.4319/lo.2009.54.5.1501
- Armstrong, R. A., C. Lee, J. I. Hedges, S. Honjo, and S. G. Wakeham. 2002. A new, mechanistic model for organic carbon fluxes in the ocean based on the quantitative association of POC with ballast minerals. *Deep. Res. Part II Top. Stud. Oceanogr.* **49**: 219–236. doi:10.1016/S0967-0645(01)00101-1
- Arrigo, K. R. 1999. Phytoplankton community structure and the drawdown of nutrients and CO₂ in the southern ocean. *Science* **283**: 365–367. doi:10.1126/science.283.5400.365
- Atkinson, A., M. J. Whitehouse, J. Priddle, G. C. Cripps, P. Ward, and M. A. Brandon. 2001. South Georgia, Antarctica: A productive, cold water, pelagic ecosystem. *Mar. Ecol. Prog. Ser.* **216**: 279–308. doi:10.3354/meps216279
- Bacon, M. P., C. A. Huh, A. P. Fleer, and W. G. Deuser. 1985. Seasonality in the flux of natural radionuclides and plutonium in the deep Sargasso Sea. *Deep Sea Res. A Oceanogr. Res. Pap.* **32**: 273–286. doi:10.1016/0198-0149(85)90079-2
- Baker, C. A., S. A. Henson, E. L. Cavan, and others. 2017. Slow-sinking particulate organic carbon in the Atlantic Ocean: Magnitude, flux, and potential controls. *Global Biogeochem. Cycles* **31**: 1051–1065. doi:10.1002/2017GB005638
- Baltar, F., J. Aristegui, J. M. Gasol, E. Sintes, and G. J. Herndl. 2009. Evidence of prokaryotic metabolism on suspended particulate organic matter in the dark waters of the subtropical North Atlantic. *Limnol. Oceanogr.* **54**: 182–193. doi:10.4319/lo.2009.54.1.0182
- Baltar, F., J. Aristegui, E. Sintes, J. M. Gasol, T. Reinthaler, and G. J. Herndl. 2010. Significance of non-sinking particulate organic carbon and dark CO₂ fixation to heterotrophic carbon demand in the mesopelagic northeast Atlantic. *Geophys. Res. Lett.* **37**: 1–6. doi:10.1029/2010GL043105
- Bannon, C. C., and D. A. Campbell. 2017. Sinking towards destiny: High throughput measurement of phytoplankton sinking rates through time-resolved fluorescence plate spectroscopy. *PLoS One* **12**: 1–16. doi:10.1371/journal.pone.0185166
- Belcher, A., M. Iversen, S. Giering, V. Riou, S. A. Henson, L. Berline, L. Guilloux, and R. Sanders. 2016. Depth-resolved particle-associated microbial respiration in the northeast Atlantic. *Biogeosciences* **13**: 4927–4943. doi:10.5194/bg-13-4927-2016
- Belcher, A., M. Iversen, C. Manno, S. A. Henson, G. A. Tarling, and R. Sanders. 2016b. The role of particle associated microbes in remineralization of fecal pellets in the upper mesopelagic of the Scotia Sea, Antarctica. *Limnol. Oceanogr.* **61**: 1049–1064. doi:10.1002/lno.10269
- Berdjeb, L., A. Parada, D. M. Needham, and J. A. Fuhrman. 2018. Short-term dynamics and interactions of marine protist communities during the spring-summer transition. *ISME J.* **12**: 1907–1917. doi:10.1038/s41396-018-0097-x
- Biard, T., E. Bigeard, S. Audic, J. Poulain, A. Gutierrez-Rodriguez, S. Pesant, L. Stemmann, and F. Not. 2017. Biogeography and diversity of Collodaria (Radiolaria) in the global ocean. *ISME J.* **11**: 1331–1344. doi:10.1038/ismej.2017.12
- Biard, T., J. W. Krause, M. R. Stukel, and M. D. Ohman. 2018. The significance of giant phaeodarians (Rhizaria) to biogenic silica export in the California current ecosystem. *Global Biogeochem. Cycles* **32**: 987–1004. doi:10.1029/2018GB005877
- Biard, T., and others. 2016. In situ imaging reveals the biomass of giant protists in the global ocean. *Nature* **532**: 504–507. doi:10.1038/nature17652
- Bishop, J. K. B., J. M. Edmond, D. R. Ketten, M. P. Bacon, and W. B. Silker. 1977. The chemistry, biology, and vertical flux of particulate matter from the upper 400 m of the equatorial Atlantic Ocean. *Deep Sea Res.* **24**: 511–548. doi:10.1016/0146-6291(77)90526-4
- Bochdansky, A. B., H. M. van Aken, and G. J. Herndl. 2010. Role of macroscopic particles in deep-sea oxygen consumption. *Proc. Natl. Acad. Sci. USA* **107**: 8287–8291. doi:10.1073/pnas.0913744107
- Bochdansky, A. B., M. A. Clouse, and G. J. Herndl. 2017. Eukaryotic microbes, principally fungi and labyrinthulomycetes, dominate biomass on bathypelagic marine snow. *ISME J.* **11**: 362–373. doi:10.1038/ismej.2016.113
- Boltovskoy, D., and N. Correa. 2016. Biogeography of Radiolaria Polycystina (Protista) in the World Ocean. *Prog. Oceanogr.* **149**: 82–105. doi:10.1016/j.pocan.2016.09.006

- Boyd, P. W., and T. W. Trull. 2007. Understanding the export of biogenic particles in oceanic waters: Is there consensus? *Prog. Oceanogr.* **72**: 276–312. doi:[10.1016/j.pocean.2006.10.007](https://doi.org/10.1016/j.pocean.2006.10.007)
- Brown, M. V., and J. P. Bowman. 2001. A molecular phylogenetic survey of sea-ice microbial communities (SIMCO). *FEMS Microbiol. Ecol.* **35**: 267–275. doi:[10.1016/S0168-6496\(01\)00100-3](https://doi.org/10.1016/S0168-6496(01)00100-3)
- Buesseler, K. O., and P. W. Boyd. 2009. Shedding light on processes that control particle export and flux attenuation in the twilight zone of the open ocean. *Limnol. Oceanogr.* **54**: 1210–1232. doi:[10.4319/lo.2009.54.4.1210](https://doi.org/10.4319/lo.2009.54.4.1210)
- Calbet, A., and M. R. Landry. 2004. Phytoplankton growth, microzooplankton grazing, and carbon cycling in marine systems. *Limnol. Oceanogr.* **49**: 51–57. doi:[10.4319/lo.2004.49.1.0051](https://doi.org/10.4319/lo.2004.49.1.0051)
- Caporaso, J. G., C. L. Lauber, W. A. Walters, D. Berg-lyons, C. A. Lozupone, P. J. Turnbaugh, N. Fierer, and R. Knight. 2010. Global patterns of 16S rRNA diversity at a depth of millions of sequences per sample. *Proc. Natl. Acad. Sci. USA* **108**: 4516–4522. doi:[10.1073/pnas.1000080107/-/DCSupplemental.www.pnas.org/cgi/doi/10.1073/pnas.1000080107](https://doi.org/10.1073/pnas.1000080107/-/DCSupplemental.www.pnas.org/cgi/doi/10.1073/pnas.1000080107)
- Caron, D. A. 2017. Acknowledging and incorporating mixed nutrition into aquatic protistan ecology, finally. *Environ. Microbiol. Rep.* **9**: 41–43. doi:[10.1111/1758-2229.12514](https://doi.org/10.1111/1758-2229.12514)
- Caron, D. A., P. D. Countway, A. C. Jones, D. Y. Kim, and A. Schnetzer. 2012. Marine Protistan Diversity. *Ann. Rev. Mar. Sci.* **4**: 467–493. doi:[10.1146/annurev-marine-120709-142802](https://doi.org/10.1146/annurev-marine-120709-142802)
- Caron, D. A., P. G. Davis, L. P. Madin, and J. M. Sieburth. 1982. Heterotrophic bacteria and bacterivorous protozoa in oceanic macroaggregates. *Science* **218**: 795–797. doi:[10.1126/science.218.4574.795](https://doi.org/10.1126/science.218.4574.795)
- Caron, D. A., R. J. Gast, and M. È. Garneau. 2016. Sea ice as a habitat for micrograzers, p. 370–393. *In* *Sea Ice*, 3rd ed. John Wiley & Sons. doi:[10.1002/9781118778371.ch15](https://doi.org/10.1002/9781118778371.ch15)
- Cassar, N., S. W. Wright, P. G. Thomson, and others. 2015. The relation of mixed-layer net community production to phytoplankton community composition in the Southern Ocean. *Global Biogeochem. Cycles* **29**: 446–462. doi:[10.1002/2014GB004936](https://doi.org/10.1002/2014GB004936)
- Cavan, E. L., F. A. C. Le Moigne, a. J. Poulton, G. a. Tarling, P. Ward, C. J. Daniels, G. M. Fragoso, and R. J. Sanders. 2015. Attenuation of particulate organic carbon flux in the Scotia Sea, Southern Ocean, is controlled by zooplankton fecal pellets. *Geophys. Res. Lett.* **42**: 821–830. doi:[10.1002/2014GL062744](https://doi.org/10.1002/2014GL062744)
- Cavan, E. L., M. Trimmer, F. Shelley, and R. Sanders. 2017. Remineralization of particulate organic carbon in an ocean oxygen minimum zone. *Nat. Commun.* **8**: 1–9. doi:[10.1038/ncomms14847](https://doi.org/10.1038/ncomms14847)
- Chen, B., and E. A. Laws. 2017. Is there a difference of temperature sensitivity between marine phytoplankton and heterotrophs? *Limnol. Oceanogr.* **62**: 806–817. doi:[10.1002/lno.10462](https://doi.org/10.1002/lno.10462)
- Cho, B. C., and F. Azam. 1988. Major role of bacteria in biogeochemical fluxes in the ocean's interior. *Nature* **332**: 441–443. doi:[10.1038/332441a0](https://doi.org/10.1038/332441a0)
- Cleary, A. C., and E. G. Durbin. 2016. Unexpected prevalence of parasite 18S rDNA sequences in winter among Antarctic marine protists. *J. Plankton Res.* **38**: 401–417. doi:[10.1093/plankt/fbw005](https://doi.org/10.1093/plankt/fbw005)
- Collins, J. R., B. R. Edwards, K. Thamatrakoln, J. E. Ossolinski, G. R. DiTullio, K. D. Bidle, S. C. Doney, and B. A. S. Van Mooy. 2015. The multiple fates of sinking particles in the North Atlantic Ocean. *Global Biogeochem. Cycles* **29**: 1471–1494. doi:[10.1002/2014GB005037](https://doi.org/10.1002/2014GB005037)
- Countway, P. D., R. J. Gast, P. Savai, and D. A. Caron. 2005. Protistan diversity estimates based on 18S rDNA from seawater incubations in the Western North Atlantic. *J. Eukaryot. Microbiol.* **52**: 95–106. doi:[10.1111/j.1550-7408.2005.05202006.x](https://doi.org/10.1111/j.1550-7408.2005.05202006.x)
- Crespo, B. G., T. Pommier, B. Fernández-Gómez, and C. Pedrós-Alió. 2013. Taxonomic composition of the particle-attached and free-living bacterial assemblages in the Northwest Mediterranean Sea analyzed by pyrosequencing of the 16S rRNA. *Microbiologyopen* **2**: 541–552. doi:[10.1002/mbo3.92](https://doi.org/10.1002/mbo3.92)
- Dall'Olmo, G., and K. A. Mork. 2014. Carbon export by small particles in the Norwegian Sea. *Geophys. Res. Lett.* **41**: 2921–2927. doi:[10.1002/2014GL059244](https://doi.org/10.1002/2014GL059244)
- Decelle, J., and others. 2013. Diversity, ecology and biogeochemistry of cyst-forming acantharia (Radiolaria) in the oceans. *PLoS One* **8**: e53598. doi:[10.1371/journal.pone.0053598](https://doi.org/10.1371/journal.pone.0053598)
- Decelle, J., and others. 2012. An original mode of symbiosis in open ocean plankton. *Proc. Natl. Acad. Sci. USA* **109**: 18000–18005. doi:[10.1073/pnas.1212303109](https://doi.org/10.1073/pnas.1212303109)
- Delong, E. F., D. G. Franks, and A. L. Alldredge. 1993. Phylogenetic diversity of aggregate-attached vs. free-living marine bacterial assemblages. *Limnol. Oceanogr.* **38**: 924–934. doi:[10.4319/lo.1993.38.5.0924](https://doi.org/10.4319/lo.1993.38.5.0924)
- DiTullio, G. R., and others. 2000. Rapid and early export of *Phaeocystis antarctica* blooms in the Ross Sea, Antarctica. *Nature* **404**: 595–598. doi:[10.1038/35007061](https://doi.org/10.1038/35007061)
- Djurhuus, A., K. Pitz, N. A. Sawaya, J. Rojas-Márquez, B. Michaud, E. Montes, F. Muller-Karger, and M. Breitbart. 2018. Evaluation of marine zooplankton community structure through environmental DNA metabarcoding. *Limnol. Oceanogr.: Methods* **16**: 209–221. doi:[10.1002/lom3.10237](https://doi.org/10.1002/lom3.10237)
- Dolan, J. R., M. Ciobanu, S. Marro, and L. Coppola. 2017. An exploratory study of heterotrophic protists of the mesoepelagic Mediterranean Sea. *ICES J. Mar. Sci.* **76**: 616–625. doi:[10.1093/icesjms/fsx218](https://doi.org/10.1093/icesjms/fsx218)
- Dolven, J. K., C. Lindqvist, V. A. Albert, K. R. Bjørklund, T. Yuasa, O. Takahashi, and S. Mayama. 2007. Molecular diversity of alveolates associated with neritic North Atlantic radiolarians. *Protist* **158**: 65–76. doi:[10.1016/j.protis.2006.07.004](https://doi.org/10.1016/j.protis.2006.07.004)

- Doolittle, D. F., W. K. W. Li, and A. M. Wood. 2008. Winter-time abundance of picoplankton in the Atlantic sector of the Southern Ocean. *Nov. Hedwigia* **133**: 147–160 doi:1438-9134/08/0133–147.
- Duret, M. T., R. S. Lampitt, and P. Lam. 2018. Prokaryotic niche partitioning between suspended and sinking marine particles. *Environ. Microbiol. Rep.* **11**: 386–400. doi:10.1111/1758-2229.12692
- Duret, M. T., M. G. Pachiadaki, F. J. Stewart, N. Sarode, U. Christaki, S. Monchy, A. Srivastava, and V. P. Edgcomb. 2015. Size-fractionated diversity of eukaryotic microbial communities in the Eastern Tropical North Pacific oxygen minimum zone. *FEMS Microbiol. Ecol.* **91**: fiv037–fiv037. doi:10.1093/femsec/fiv037
- Dziallas, C., M. Allgaier, M. T. Monaghan, and H. P. Grossart. 2012. Act together—implications of symbioses in aquatic ciliates. *Front. Microbiol.* **3**: 1–17. doi:10.3389/fmicb.2012.00288
- Eberlein, K., M. Leal, K. Hammer, and W. Hickel. 1985. Dissolved organic substances during a *Phaeocystis pouchetii* bloom in the German Bight (North Sea). *Mar. Biol.* **316**: 311–316. doi:10.1038/470444a
- Ebersbach, F., T. W. Trull, D. M. Davies, and S. G. Bray. 2011. Controls on mesopelagic particle fluxes in the Sub-Antarctic and Polar Frontal Zones in the Southern Ocean south of Australia in summer—Perspectives from free-drifting sediment traps. *Deep. Res. Part II Top. Stud. Oceanogr.* **58**: 2260–2276. doi:10.1016/j.dsr2.2011.05.025
- Edgcomb, V., and others. 2011. Protistan microbial observatory in the Cariaco Basin, Caribbean. I. Pyrosequencing vs Sanger insights into species richness. *ISME J.* **5**: 1344–1356. doi:10.1038/ismej.2011.6
- Edgcomb, V. P. 2016. Marine protist associations and environmental impacts across trophic levels in the twilight zone and below. *Curr. Opin. Microbiol.* **31**: 169–175. doi:10.1016/j.mib.2016.04.001
- Fenchel, T. 1982a. Ecology of heterotrophic microflagellates. I. Some important forms and their functional morphology. *Mar. Ecol. Prog. Ser. Oldend.* **8**: 211–223.
- Fenchel, T. 1982b. Ecology of heterotrophic microflagellates. II. Bioenergetics and growth. *Mar. Ecol. Prog. Ser.* **8**: 225–231.
- Fenchel, T. 1982c. Ecology of heterotrophic microflagellates. III. Adaptations to heterogeneous environments. *Mar. Ecol. Prog. Ser.* **9**: 25–33.
- Fenchel, T. 2001. How dinoflagellates swim. *Protist* **152**: 329–338. doi:10.1078/1434-4610-00071
- Flaviani, F., D. Schroeder, C. Balestreri, J. Schroeder, K. Moore, K. Paszkiewicz, M. Pfaff, and E. Rybicki. 2017. A Pelagic Microbiome (Viruses to Protists) from a Small Cup of Seawater. *Viruses* **9**: 47. doi:10.3390/v9030047
- Flynn, K. J., D. K. Stoecker, A. Mitra, J. A. Raven, P. M. Glibert, P. J. Hansen, E. Granéli, and J. M. Burkholder. 2013. Misuse of the phytoplankton-zooplankton dichotomy: The need to assign organisms as mixotrophs within plankton functional types. *J. Plankton Res.* **35**: 3–11. doi:10.1093/plankt/fbs062
- Francois, R., S. Honjo, R. Krishfield, and S. Manganini. 2002. Factors controlling the flux of organic carbon to the bathypelagic zone of the ocean. *Global Biogeochem. Cycles* **16**: 34–1–34–20. doi:10.1029/2001GB001722
- Garrison, D. L., A. Gibson, S. L. Coale, M. M. Gowing, Y. B. Okolodkov, C. H. Fritsen, and M. O. Jeffries. 2005. Sea-ice microbial communities in the Ross Sea: Autumn and summer biota. *Mar. Ecol. Prog. Ser.* **300**: 39–52. doi:10.3354/meps300039
- Garzio, L. M., D. K. Steinberg, M. Erickson, and H. W. Ducklow. 2013. Microzooplankton grazing along the Western Antarctic Peninsula. *Aquat. Microb. Ecol.* **70**: 215–232. doi:10.3354/ame01655
- Georges, C., S. Monchy, S. Genitsaris, and U. Christaki. 2014. Protist community composition during early phytoplankton blooms in the naturally iron-fertilized Kerguelen area (Southern Ocean). *Biogeosci. Discuss.* **11**: 11179–11215. doi:10.5194/bgd-11-11179-2014
- Giering, S. L. C., and others. 2014. Reconciliation of the carbon budget in the ocean's twilight zone. *Nature* **507**: 480–483. doi:10.1038/nature13123
- Giering, S. L. C., R. Sanders, A. P. Martin, S. A. Henson, J. S. Riley, C. M. Marsay, and D. G. Johns. 2017. Particle flux in the oceans: Challenging the steady state assumption. *Global Biogeochem. Cycles* **31**: 159–171. doi:10.1002/2016GB005424
- Giesecke, R., H. E. González, and U. Bathmann. 2010. The role of the chaetognath *Sagitta gazellae* in the vertical carbon flux of the Southern Ocean. *Polar Biol.* **33**: 293–304. doi:10.1007/s00300-009-0704-4
- Gloeckler, K., C. A. Choy, C. C. S. Hannides, H. G. Close, E. Goetze, B. N. Popp, and J. C. Drazen. 2017. Stable isotope analysis of micronekton around Hawaii reveals suspended particles are an important nutritional source in the lower mesopelagic and upper bathypelagic zones. *Limnol. Oceanogr.* **63**: 1168–1180. doi:10.1002/lno.10762
- Godhe, A., M. E. Asplund, K. Hämström, V. Saravanan, A. Tyagi, and I. Karunasagar. 2008. Quantification of diatom and dinoflagellate biomasses in coastal marine seawater samples by real-time PCR. *Appl. Environ. Microbiol.* **74**: 7174–7182. doi:10.1128/AEM.01298-08
- Gómez, F., D. Moreira, and P. López-García. 2009. Life cycle and molecular phylogeny of the dinoflagellates chytridinium and dissodinium, ectoparasites of copepod eggs. *Eur. J. Protistol.* **45**: 260–270. doi:10.1016/j.ejop.2009.05.004
- Gonçalves, V. N., A. B. M. Vaz, C. A. Rosa, and L. H. Rosa. 2012. Diversity and distribution of fungal communities in lakes of Antarctica. *FEMS Microbiol. Ecol.* **82**: 459–471. doi:10.1111/j.1574-6941.2012.01424.x
- Gong, J., J. Dong, X. Liu, and R. Massana. 2013. Extremely high copy numbers and polymorphisms of the rDNA operon estimated from single cell analysis of oligotrich and

- peritrich ciliates. *Protist* **164**: 369–379. doi:[10.1016/j.protis.2012.11.006](https://doi.org/10.1016/j.protis.2012.11.006)
- Gowing, M. M., D. L. Garrison, H. B. Kunze, and C. J. Winchell. 2001. Biological components of Ross Sea short-term particle fluxes in the austral summer of 1995–1996. *Deep. Res. Part I Oceanogr. Res. Pap.* **48**: 2645–2671. doi:[10.1016/S0967-0637\(01\)00034-6](https://doi.org/10.1016/S0967-0637(01)00034-6)
- Gowing, M. M., D. L. Garrison, K. F. Wishner, and C. Gelfman. 2003. Mesopelagic microplankton of the Arabian Sea. *Deep. Res. Part I Oceanogr. Res. Pap.* **50**: 1205–1234. doi:[10.1016/S0967-0637\(03\)00130-4](https://doi.org/10.1016/S0967-0637(03)00130-4)
- Gowing, M. M., and M. W. Silver. 1985. Minipellets: A new and abundant size class of marine fecal pellets. *J. Mar. Res.* **43**: 395–418. doi:[10.1357/002224085788438676](https://doi.org/10.1357/002224085788438676)
- Grattepanche, J.-D., L. F. Santoferrara, G. B. McManus, and L. A. Katz. 2016. Unexpected biodiversity of ciliates in marine samples from below the photic zone. *Mol. Ecol.* **25**: 3987–4000. doi:[10.1111/mec.13745](https://doi.org/10.1111/mec.13745)
- Grossart, H.-P., S. Van den Wyngaert, M. Kagami, C. Wurzbacher, M. Cunliffe, and K. Rojas-Jimenez. 2019. Fungi in aquatic ecosystems. *Nat. Rev. Microbiol.* **17**: 339–354. doi:[10.1038/s41579-019-0175-8](https://doi.org/10.1038/s41579-019-0175-8)
- Guillou, L., and others. 2012. The Protist Ribosomal Reference database (PR2): a catalog of unicellular eukaryote Small Sub-Unit rRNA sequences with curated taxonomy. *Nucleic Acids Res.* **41**: D597–D604. doi:[10.1093/nar/gks1160](https://doi.org/10.1093/nar/gks1160)
- Guillou, L., M. Viprey, A. Chambouvet, R. M. Welsh, A. R. Kirkham, R. Massana, D. J. Scanlan, and A. Z. Worden. 2008. Widespread occurrence and genetic diversity of marine parasitoids belonging to Syndiniales (*Alveolata*). *Environ. Microbiol.* **10**: 3349–3365. doi:[10.1111/j.1462-2920.2008.01731.x](https://doi.org/10.1111/j.1462-2920.2008.01731.x)
- Gutierrez-Rodriguez, A., M. R. Stukel, A. Lopes dos Santos, T. Biard, R. Scharek, D. Vaultot, M. R. Landry, and F. Not. 2019. High contribution of Rhizaria (Radiolaria) to vertical export in the California Current Ecosystem revealed by DNA metabarcoding. *ISME J.* **13**: 964–976. doi:[10.1038/s41396-018-0322-7](https://doi.org/10.1038/s41396-018-0322-7)
- Gutiérrez, M. H., S. Pantoja, R. A. Quiñones, and R. R. González. 2010. First record of filamentous fungi in the coastal upwelling ecosystem off central Chile Primer registro de hongos filamentosos en el ecosistema de surgencia costero frente a Chile central. *Gayana* **74**: 66–73.
- Gutiérrez, M. H., S. Pantoja, E. Tejos, and R. A. Quiñones. 2011. The role of fungi in processing marine organic matter in the upwelling ecosystem off Chile. *Mar. Biol.* **158**: 205–219. doi:[10.1007/s00227-010-1552-z](https://doi.org/10.1007/s00227-010-1552-z)
- Hadziavdic, K., K. Lekang, A. Lanzen, I. Jonassen, E. M. Thompson, and C. Troedsson. 2014. Characterization of the 18S rRNA gene for designing universal eukaryote specific primers. *PLoS One* **9**: e87624. doi:[10.1371/journal.pone.0087624](https://doi.org/10.1371/journal.pone.0087624)
- Harada, A., S. Ohtsuka, and T. Horiguchi. 2007. Species of the parasitic genus *duboscquella* are members of the enigmatic marine alveolate group I. *Protist* **158**: 337–347. doi:[10.1016/j.protis.2007.03.005](https://doi.org/10.1016/j.protis.2007.03.005)
- Head, M. J., R. Harland, and J. Matthiessen. 2001. Cold marine indicators of the late Quaternary: The new dinoflagellate cyst genus *Islandinium* and related morphotypes. *J. Quat. Sci.* **16**: 621–636. doi:[10.1002/jqs.657](https://doi.org/10.1002/jqs.657)
- Herndl, G. J., and T. Reinthaler. 2013. Microbial control of the dark end of the biological pump. *Nat. Geosci.* **6**: 718–724. doi:[10.1038/ngeo1921](https://doi.org/10.1038/ngeo1921)
- Hoffmann, L. J., I. Peeken, and K. Lochte. 2008. Iron, silicate, and light co-limitation of three Southern Ocean diatom species. *Polar Biol.* **31**: 1067–1080. doi:[10.1007/s00300-008-0448-6](https://doi.org/10.1007/s00300-008-0448-6)
- Hong, Y., W. O. Smith, and A.-M. White. 1997. Studies on transparent exopolymer particles (Tep) produced in the Ross Sea (Antarctica) and by *Phaeocystis antarctica* (Prymnesiophyceae) 1. *J. Phycol.* **33**: 368–376. doi:[10.1111/j.0022-3646.1997.00368.x](https://doi.org/10.1111/j.0022-3646.1997.00368.x)
- Ishikawa, A., S. W. Wright, R. van den Enden, A. T. Davidson, and H. J. Marchant. 2002. Abundance, size structure and community composition of phytoplankton in the Southern Ocean in the austral summer 1999/2000. *Polar Biosci.* **15**: 11–26.
- Jacques, G. 1983. Some ecophysiological aspects of the Antarctic phytoplankton. *Polar Biol.* **2**: 27–33. doi:[10.1007/BF00258282](https://doi.org/10.1007/BF00258282)
- Jacques, G., and M. Panouse. 1991. Biomass and composition of size fractionated phytoplankton in the Weddell-Scotia Confluence area. *Polar Biol.* **11**: 315–328. doi:[10.1007/BF00239024](https://doi.org/10.1007/BF00239024)
- Jensen, M. H., and N. Daugbjerg. 2009. Molecular phylogeny of selected species of the order dinophysiales (Dinophyceae)-testing the hypothesis of a dinophysoid radiation. *J. Phycol.* **45**: 1136–1152. doi:[10.1111/j.1529-8817.2009.00741.x](https://doi.org/10.1111/j.1529-8817.2009.00741.x)
- Jeong, H. J., Y. Du Yoo, N. S. Kang, J. R. Rho, K. A. Seong, J. W. Park, G. S. Nam, and W. Yih. 2010. Ecology of *Gymnodinium aureolum*. I. Feeding in western Korean waters. *Aquat. Microb. Ecol.* **59**: 239–255. doi:[10.3354/ame01394](https://doi.org/10.3354/ame01394)
- Jiang, Y., E. J. Yang, J. O. Min, T. W. Kim, and S. H. Kang. 2015. Vertical variation of pelagic ciliate communities in the western Arctic Ocean. *Deep. Res. Part II Top. Stud. Oceanogr.* **120**: 103–113. doi:[10.1016/j.dsr2.2014.09.005](https://doi.org/10.1016/j.dsr2.2014.09.005)
- Jin, X., N. Gruber, J. P. Dune, J. L. Sarmiento, and R. A. Armstrong. 2006. Diagnosing the contributions of phytoplankton functional groups to the production and export of particulate organic carbon, CaCO₃, and opal from global nutrient and alkalinity distributions. *Global Biogeochem. Cycles* **20**: 1–17. doi:[10.1029/2005GB002532](https://doi.org/10.1029/2005GB002532)
- Kjørboe, T., and G. A. Jackson. 2001. Marine snow, organic solute plumes, and optimal chemosensory behavior of bacteria. *Limnol. Oceanogr.* **46**: 1309–1318. doi:[10.4319/lo.2001.46.6.1309](https://doi.org/10.4319/lo.2001.46.6.1309)
- Kirchman, D. L. [ed.]. 2008. *Microbial ecology of the oceans*. John Wiley & Sons, Inc.

- Klaas, C., and D. E. Archer. 2002. Association of sinking organic matter with various types of mineral ballast in the deep sea: Implications for the rain ratio. *Global Biogeochem. Cycles* **16**: 63–1–63–14. doi:10.1029/2001GB001765
- Korb, R. E., M. J. Whitehouse, P. Ward, M. Gordon, H. J. Venables, and A. J. Poulton. 2012. Regional and seasonal differences in microplankton biomass, productivity, and structure across the Scotia Sea: Implications for the export of biogenic carbon. *Deep. Res. Part II Top. Stud. Oceanogr.* **59–60**: 67–77. doi:10.1016/j.dsr2.2011.06.006
- Kwon, E. Y., F. Primeau, and J. L. Sarmiento. 2009. The impact of remineralization depth on the air–sea carbon balance. *Nat. Geosci.* **2**: 630–635. doi:10.1038/ngeo612
- De La Rocha, C. L., and U. Passow. 2007. Factors influencing the sinking of POC and the efficiency of the biological carbon pump. *Deep. Res. Part II Top. Stud. Oceanogr.* **54**: 639–658. doi:10.1016/j.dsr2.2007.01.004
- Lam, P. J., and O. Marchal. 2015. Insights into particle cycling from thorium and particle data. *Ann. Rev. Mar. Sci.* **7**: 159–184. doi:10.1146/annurev-marine-010814-015623
- Lam, P., M. M. Jensen, A. Kock, K. A. Lettmann, Y. Plancherel, G. Lavik, H. W. Bange, and M. M. M. Kuypers. 2011. Origin and fate of the secondary nitrite maximum in the Arabian Sea. *Biogeosciences* **8**: 1565–1577. doi:10.5194/bg-8-1565-2011
- Lampitt, R. S., T. Noji, and B. von Bodungen. 1990. What happens to zooplankton faecal pellets? Implications for material flux. *Mar. Biol.* **104**: 15–23. doi:10.1007/BF01313152
- Lampitt, R. S., I. Salter, and D. Johns. 2009. Radiolaria: Major exporters of organic carbon to the deep ocean. *Global Biogeochem. Cycles* **23**: 1–9. doi:10.1029/2008GB003221
- Lampitt, R. S., K. F. Wishner, C. M. Turley, and M. V. Angel. 1993. Marine snow studies in the Northeast Atlantic Ocean: Distribution, composition and role as a food source for migrating plankton. *Mar. Biol.* **116**: 689–702. doi:10.1007/BF00355486
- Leblanc, K., and others. 2018. Nanoplanktonic diatoms are globally overlooked but play a role in spring blooms and carbon export. *Nat. Commun.* **9**: 1–12. doi:10.1038/s41467-018-03376-9
- Legendre, L., and J. Le Fevre. 1995. Microbial food webs and the export of biogenic carbon in oceans. *Aquat. Microb. Ecol.* **9**: 69–77. doi:10.3354/ame009069
- Legendre, L., and F. Rassoulzadegan. 1996. Food-web mediated export of biogenic carbon in oceans. *Mar. Ecol. Prog. Ser.* **145**: 179–193.
- Lin, Y., N. Cassar, A. Marchetti, C. Moreno, H. Ducklow, and Z. Li. 2017. Specific eukaryotic plankton are good predictors of net community production in the Western Antarctic Peninsula. *Sci. Rep.* **7**: 1–11. doi:10.1038/s41598-017-14109-1
- López-García, P., F. Rodríguez-Valera, C. Pedrós-Alió, and D. Moreira. 2001. Unexpected diversity of small eukaryotes in deep-sea Antarctic plankton. *Nature* **409**: 603–607. doi:10.1038/35054537
- López-Pérez, M., A. Gonzaga, A.-B. Martín-Cuadrado, O. Onyshchenko, A. Ghavidel, R. Ghai, and F. Rodríguez-Valera. 2012. Genomes of surface isolates of *Alteromonas macleodii*: The life of a widespread marine opportunistic copiotroph. *Sci. Rep.* **2**: 696. doi:10.1038/srep00696
- Marchant, H. J. 1985. Choanoflagellates in the Antarctic marine food chain, p. 271–276. *In* Antarctic nutrient cycles and food webs. Springer Berlin Heidelberg.
- Mari, X., U. Passow, C. Mignon, A. B. Burd, and L. Legendre. 2017. Transparent exopolymer particles: Effects on carbon cycling in the ocean. *Prog. Oceanogr.* **151**: 13–37. doi:10.1016/j.pocean.2016.11.002
- Martin, J. H., G. A. Knauer, D. M. Karl, and W. W. Broenkow. 1987. VERTEX: Carbon cycling in the northeast Pacific. *Deep Sea Res. Part A. Oceanogr. Res. Pap.* **34**: 267–285. doi:10.1016/0198-0149(87)90086-0
- Masella, A. P., A. K. Bartram, J. M. Truszkowski, D. G. Brown, and J. D. Neufeld. 2012. PANDAseq: PAired-eND Assembler for Illumina sequences. *BMC Bioinformatics* **13**: 31. doi:10.1186/1471-2105-13-31
- Mayor, D. J., R. Sanders, S. L. C. Giering, and T. R. Anderson. 2014. Microbial gardening in the ocean’s twilight zone: Detritivorous metazoans benefit from fragmenting, rather than ingesting, sinking detritus. *Bioessays* **36**: 1132–1137. doi:10.1002/bies.201400100
- McDonnell, A. M. P., and others. 2015. The oceanographic toolbox for the collection of sinking and suspended marine particles. *Prog. Oceanogr.* **133**: 17–31. doi:10.1016/j.pocean.2015.01.007
- Medinger, R., V. Nolte, R. V. Pandey, S. Jost, B. Ottenwälder, C. Schlötterer, and J. Boenigk. 2010. Diversity in a hidden world: Potential and limitation of next-generation sequencing for surveys of molecular diversity of eukaryotic microorganisms. *Mol. Ecol.* **19**: 32–40. doi:10.1111/j.1365-294X.2009.04478.x
- Mestre, M., E. Borrull, M. Sala, and J. M. Gasol. 2017. Patterns of bacterial diversity in the marine planktonic particulate matter continuum. *ISME J.* **11**: 999–1010. doi:10.1038/ismej.2016.166
- Morgan-Smith, D., M. A. Clouse, G. J. Herndl, and A. B. Bochdansky. 2013. Diversity and distribution of microbial eukaryotes in the deep tropical and subtropical North Atlantic Ocean. *Deep. Res. Part I Oceanogr. Res. Pap.* **78**: 58–69. doi:10.1016/j.dsr.2013.04.010
- Okolodkov, Y. B. 1999. Species range types of recent marine dinoflagellates recorded from the Arctic. *Grana* **38**: 162–169. doi:10.1080/00173139908559224
- Orsi, W., Y. C. Song, S. Hallam, and V. Edgcomb. 2012. Effect of oxygen minimum zone formation on communities of marine protists. *ISME J.* **6**: 1586–1601. doi:10.1038/ismej.2012.7
- Pahlow, M., U. Riebesell, and D. A. Wolf-Gladrow. 1997. Impact of cell shape and chain formation on nutrient

- acquisition by marine diatoms. *Limnol. Oceanogr.* **42**: 1660–1672. doi:10.4319/lo.1997.42.8.1660
- Pakhomov, E. A., Y. Podeswa, B. P. V. Hunt, and L. E. Kwong. 2018. Vertical distribution and active carbon transport by pelagic decapods in the North Pacific Subtropical Gyre. *ICES J. Mar. Sci.* **76**: 702–717. doi:10.1093/icesjms/fsy134
- Parris, D. J., S. Ganesh, V. P. Edgcomb, E. F. DeLong, and F. J. Stewart. 2014. Microbial eukaryote diversity in the marine oxygen minimum zone off northern Chile. *Front. Microbiol.* **5**: 1–11. doi:10.3389/fmicb.2014.00543
- Passow, U., R. F. Shipe, A. Murray, D. K. Pak, M. A. Brzezinski, and A. L. Alldredge. 2001. The origin of transparent exopolymer particles (TEP) and their role in the sedimentation of particulate matter. *Cont. Shelf Res.* **21**: 327–346. doi:10.1016/S0278-4343(00)00101-1
- Pernice, M. C., and others. 2014. Global abundance of planktonic heterotrophic protists in the deep ocean. *ISME J.* **9**: 782–792. doi:10.1038/ismej.2014.168
- Pernice, M. C., C. R. Giner, R. Logares, J. Perera-Bel, S. G. Acinas, C. M. Duarte, J. M. Gasol, and R. Massana. 2016. Large variability of bathypelagic microbial eukaryotic communities across the world's oceans. *ISME J.* **10**: 945–958. doi:10.1038/ismej.2015.170
- Pernice, M. C., R. Logares, L. Guillou, and R. Massana. 2013. General patterns of diversity in major marine micro-eukaryote lineages. J.H. Badger [ed.]. *PLoS One* **8**: e57170. doi:10.1371/journal.pone.0057170
- Petrou, K., S. A. Kranz, S. Trimborn, C. S. Hassler, S. B. Ameijeiras, O. Sackett, P. J. Ralph, and A. T. Davidson. 2016. Southern Ocean phytoplankton physiology in a changing climate. *J. Plant Physiol.* **203**: 135–150. doi:10.1016/j.jplph.2016.05.004
- Ploug, H., and H.-P. Grossart. 2000. Bacterial growth and grazing on diatom aggregates: Respiratory carbon turnover as a function of aggregate size and sinking velocity. *Limnol. Oceanogr.* **45**: 1467–1475. doi:10.4319/lo.2000.45.7.1467
- Ploug, H., M. H. Iversen, and G. Fischer. 2008. Ballast, sinking velocity, and apparent diffusivity within marine snow and zooplankton fecal pellets: Implications for substrate turnover by attached bacteria. *Limnol. Oceanogr.* **53**: 1878–1886. doi:10.4319/lo.2008.53.5.1878
- Pomeroy, L. R., and W. J. Wiebe. 1988. Energetics of microbial food webs. *Hydrobiologia* **159**: 7–18. doi:10.1007/BF0007363
- Poulsen, L. K., and M. H. Iversen. 2008. Degradation of copepod fecal pellets: Key role of protozooplankton. *Mar. Ecol. Prog. Ser.* **367**: 1–13. doi:10.3354/meps07611
- Poulton, R. E. K., M. J. Whitehouse, M. Gordon, P. Ward, and A.J. 2010. Summer microplankton community structure across the Scotia Sea: Implications for biological carbon export. *Biogeosciences* **7**: 343–346.
- Quast, C., E. Pruesse, P. Yilmaz, J. Gerken, T. Schweer, P. Yarza, J. Peplies, and F. O. Glöckner. 2013. The SILVA ribosomal RNA gene database project: Improved data processing and web-based tools. *Nucleic Acids Res.* **41**: 590–596. doi:10.1093/nar/gks1219
- Rembauville, M., C. Manno, G. A. Tarling, S. Blain, and I. Salter. 2016. Strong contribution of diatom resting spores to deep-sea carbon transfer in naturally iron-fertilized waters downstream of South Georgia. *Deep Sea Res. Part I Oceanogr. Res. Pap.* **115**: 22–35. doi:10.1016/j.dsr.2016.05.002
- Riley, J. S., R. Sanders, C. Marsay, F. A. C. Le Moigne, E. P. Achterberg, and A. J. Poulton. 2012. The relative contribution of fast and slow sinking particles to ocean carbon export. *Global Biogeochem. Cycles* **26**: n/a–n/a. doi:10.1029/2011GB004085
- Rodríguez-Marconi, S., R. De La Iglesia, B. Díez, C. A. Fonseca, E. Hajdu, N. Trefault, and N. Webster. 2015. Characterization of bacterial, archaeal and eukaryote symbionts from antarctic sponges reveals a high diversity at a three-domain level and a particular signature for this ecosystem. *PLoS One* **10**: 1–19. doi:10.1371/journal.pone.0138837
- Rojas-Jimenez, K., C. Wurzbacher, E. C. Bourne, A. Chiuchiolo, J. C. Priscu, and H. P. Grossart. 2017. Early diverging lineages within Cryptomycota and Chytridiomycota dominate the fungal communities in ice-covered lakes of the McMurdo Dry Valleys. *Antarctica. Sci. Rep.* **7**: 1–11. doi:10.1038/s41598-017-15598-w
- Safi, K. A., K. V. Robinson, J. A. Hall, J. Schwarz, and E. W. Maas. 2012. Ross Sea deep-ocean and epipelagic microzooplankton during the summer-autumn transition period. *Aquat. Microb. Ecol.* **67**: 123–137. doi:10.3354/ame01588
- Sauvadet, A. L., A. Gobet, and L. Guillou. 2010. Comparative analysis between protist communities from the deep-sea pelagic ecosystem and specific deep hydrothermal habitats. *Environ. Microbiol.* **12**: 2946–2964. doi:10.1111/j.1462-2920.2010.02272.x
- Schmoker, C., S. Hernández-León, and A. Calbet. 2013. Microzooplankton grazing in the oceans: Impacts, data variability, knowledge gaps and future directions. *J. Plankton Res.* **35**: 691–706. doi:10.1093/plankt/fbt023
- Sedwick, P. N., and G. R. Ditullio. 1997. Regulation of algal blooms in Antarctic shelf waters by the release of iron from melting sea ice. *Geophys. Res. Lett.* **24**: 2515–2518. doi:10.1029/97GL02596
- Sherr, E. B., and B. F. Sherr. 2002. Significance of predation by protists. *Antonie Van Leeuwenhoek* **81**: 293–308.
- Sherr, E. B., and B. F. Sherr. 2007. Heterotrophic dinoflagellates: A significant component of microzooplankton biomass and major grazers of diatoms in the sea. *Mar. Ecol. Prog. Ser.* **352**: 187–197. doi:10.3354/meps07161
- Silver, M. W., S. L. Coale, C. H. Pilskaln, and D. R. Steinberg. 1998. Giant aggregates: Importance as microbial centers and agents of material flux in the mesopelagic zone. *Limnol. Oceanogr.* **43**: 498–507. doi:10.4319/lo.1998.43.3.0498

- Simon, M., H. P. Grossart, B. Schweitzer, and H. Ploug. 2002. Microbial ecology of organic aggregates in aquatic ecosystems. *Aquat. Microb. Ecol.* **28**: 175–211. doi:[10.3354/ame028175](https://doi.org/10.3354/ame028175)
- Skovgaard, A., S. A. Karpov, and L. Guillou. 2012. The parasitic dinoflagellates *Blastodinium* spp. Inhabiting the gut of marine, Planktonic copepods: Morphology, ecology, and unrecognized species diversity. *Front. Microbiol.* **3**: 1–22. doi:[10.3389/fmicb.2012.00305](https://doi.org/10.3389/fmicb.2012.00305)
- Skovgaard, A., R. Massana, V. Balagué, and E. Saiz. 2005. Phylogenetic position of the copepod-infesting parasite *Syndinium turbo* (Dinoflagellata, Syndinea). *Protist* **156**: 413–423. doi:[10.1016/j.protis.2005.08.002](https://doi.org/10.1016/j.protis.2005.08.002)
- Smetacek, V., C. Klaas, S. Menden-Deuer, and T. A. Ryneerson. 2002. Mesoscale distribution of dominant diatom species relative to the hydrographical field along the Antarctic Polar Front. *Deep. Res. Part II Top. Stud. Oceanogr.* **49**: 3835–3848. doi:[10.1016/S0967-0645\(02\)00113-3](https://doi.org/10.1016/S0967-0645(02)00113-3)
- Smith, D. C., M. Simon, A. L. Alldredge, and F. Azam. 1992. Intense hydrolytic enzyme activity on marine aggregates and implications for rapid particle dissolution. *Nature* **359**: 139–142. doi:[10.1038/359139a0](https://doi.org/10.1038/359139a0)
- Smith, W. O., A. R. Shields, J. C. Dreyer, J. A. Peloquin, and V. Asper. 2011. Interannual variability in vertical export in the Ross Sea: Magnitude, composition, and environmental correlates. *Deep. Res. Part I Oceanogr. Res. Pap.* **58**: 147–159. doi:[10.1016/j.dsr.2010.11.007](https://doi.org/10.1016/j.dsr.2010.11.007)
- Stamieszkin, K., N. Poulton, and A. Pershing. 2017. Zooplankton grazing and egestion shifts particle size distribution in natural communities. *Mar. Ecol. Prog. Ser.* **575**: 43–56. doi:[10.3354/meps12212](https://doi.org/10.3354/meps12212)
- Steinberg, D. K., C. A. Carlson, N. R. Bates, S. A. Goldthwait, L. P. Madin, and A. F. Michaels. 2000. Zooplankton vertical migration and the active transport of dissolved organic and inorganic carbon in the Sargasso Sea. *Deep. Res. Part I Oceanogr. Res. Pap.* **47**: 137–158. doi:[10.1016/S0967-0637\(99\)00052-7](https://doi.org/10.1016/S0967-0637(99)00052-7)
- Steinberg, D. K., and M. R. Landry. 2017. Zooplankton and the ocean carbon cycle. *Ann. Rev. Mar. Sci.* **9**: 413–444. doi:[10.1146/annurev-marine-010814-015924](https://doi.org/10.1146/annurev-marine-010814-015924)
- Steinberg, D. K., B. A. S. Van Mooy, K. O. Buesseler, P. W. Boyd, T. Kobari, and D. M. Karl. 2008. Bacterial vs. zooplankton control of sinking particle flux in the ocean's twilight zone. *Limnol. Oceanogr.* **53**: 1327–1338. doi:[10.4319/lo.2008.53.4.1327](https://doi.org/10.4319/lo.2008.53.4.1327)
- Stoecker, D. K., P. J. Hansen, D. A. Caron, and A. Mitra. 2017. Mixotrophy in the marine plankton. *Ann. Rev. Mar. Sci.* **9**: 311–335. doi:[10.1146/annurev-marine-010816-060617](https://doi.org/10.1146/annurev-marine-010816-060617)
- Strom, S. L., R. Benner, S. Ziegler, and M. J. Dagg. 1997. Planktonic grazers are a potentially important source of marine dissolved organic carbon. *Limnol. Oceanogr.* **42**: 1364–1374.
- Stukel, M. R., T. Biard, J. Krause, and M. D. Ohman. 2018. Large Phaeodaria in the twilight zone: Their role in the carbon cycle. *Limnol. Oceanogr.* **63**: 2579–2594. doi:[10.1002/lno.10961](https://doi.org/10.1002/lno.10961)
- Suzuki, N., and Y. Aita. 2011. Radiolaria: Achievements and unresolved issues: Taxonomy and cytology. *Plankt. Benthos Res.* **6**: 69–91. doi:[10.3800/pbr.6.69](https://doi.org/10.3800/pbr.6.69)
- Suzuki, N., and F. Not. 2015. Biology and ecology of radiolaria, p. 179–222. *In* S. Ohtsuka, T. Suzuki, T. Horiguchi, N. Suzuki, and F. Not [eds.], *Marine protists: Diversity and dynamics*. Springer.
- Tanaka, T., and F. Rassoulzadegan. 2002. Full-depth profile (0–2000 m) of bacteria, heterotrophic nanoflagellates and ciliates in the NW Mediterranean Sea: Vertical partitioning of microbial trophic structures. *Deep Sea Res. Part II Top. Stud. Oceanogr.* **49**: 2093–2107. doi:[10.1016/S0967-0645\(02\)00029-2](https://doi.org/10.1016/S0967-0645(02)00029-2)
- Taylor, G. T., and C. W. Sullivan. 2008. Vitamin B12 and cobalt cycling among diatoms and bacteria in Antarctic sea ice microbial communities. *Limnol. Oceanogr.* **53**: 1862–1877. doi:[10.4319/lo.2008.53.5.1862](https://doi.org/10.4319/lo.2008.53.5.1862)
- Taylor, J. D., and M. Cunliffe. 2016. Multi-year assessment of coastal planktonic fungi reveals environmental drivers of diversity and abundance. *ISME J.* **10**: 1–11. doi:[10.1038/ismej.2016.24](https://doi.org/10.1038/ismej.2016.24)
- Thomsen, H. a., K. R. Buck, P. A. Bolt, and D. L. Garrison. 1991. Fine structure and biology of *Cryothecomonas* gen. nov. (Protista incertae sedis) from the ice biota. *Can. J. Zool.* **69**: 1048–1070. doi:[10.1139/z91-150](https://doi.org/10.1139/z91-150)
- Thomsen, P. F., J. Kielgast, L. L. Iversen, P. R. Møller, M. Rasmussen, and E. Willerslev. 2012. Detection of a diverse marine fish fauna using environmental DNA from seawater samples. *PLoS One* **7**: 1–9. doi:[10.1371/journal.pone.0041732](https://doi.org/10.1371/journal.pone.0041732)
- Tréguer, P., and others. 2018. Influence of diatom diversity on the ocean biological carbon pump. *Nat. Geosci.* **11**: 27–37. doi:[10.1038/s41561-017-0028-x](https://doi.org/10.1038/s41561-017-0028-x)
- Turner, J. T. 2015. Zooplankton fecal pellets, marine snow, phytodetritus and the ocean's biological pump. *Prog. Oceanogr.* **130**: 205–248. doi:[10.1016/j.pocean.2014.08.005](https://doi.org/10.1016/j.pocean.2014.08.005)
- de Vargas, C., and others. 2015. Ocean plankton. Eukaryotic plankton diversity in the sunlit ocean. *Science* **348**: 1261605. doi:[10.1126/science.1261605](https://doi.org/10.1126/science.1261605)
- Verdugo, P., A. L. Alldredge, F. Azam, D. L. Kirchman, U. Passow, and P. H. Santschi. 2004. The oceanic gel phase: A bridge in the DOM-POM continuum. *Mar. Chem.* **92**: 67–85. doi:[10.1029/2002GL016046](https://doi.org/10.1029/2002GL016046)
- Viprey, M., L. Guillou, M. Ferréol, and D. Vaulot. 2008. Wide genetic diversity of picoplanktonic green algae (Chloroplastida) in the Mediterranean Sea uncovered by a phylum-biased PCR approach. *Environ. Microbiol.* **10**: 1804–1822. doi:[10.1111/j.1462-2920.2008.01602.x](https://doi.org/10.1111/j.1462-2920.2008.01602.x)
- Williams, R. A. J., H. L. Owens, J. Clamp, A. T. Peterson, A. Warren, and M. Martín-Cereceda. 2018. Endemicity and climatic niche differentiation in three marine ciliated protists. *Limnol. Oceanogr.* **63**: 2727–2736. doi:[10.1002/lno.11003](https://doi.org/10.1002/lno.11003)

- Wilson, S. E., D. K. Steinberg, and K. O. Buesseler. 2008. Changes in fecal pellet characteristics with depth as indicators of zooplankton repackaging of particles in the mesopelagic zone of the subtropical and subarctic North Pacific Ocean. *Deep. Res. Part II Top. Stud. Oceanogr.* **55**: 1636–1647. doi:[10.1016/j.dsr2.2008.04.019](https://doi.org/10.1016/j.dsr2.2008.04.019)
- Worden, A. Z., M. J. Follows, S. J. Giovannoni, S. Wilken, A. E. Zimmerman, and P. J. Keeling. 2015. Rethinking the marine carbon cycle: Factoring in the multifarious lifestyles of microbes. *Science* **347**: 1257594–1257594. doi:[10.1126/science.1257594](https://doi.org/10.1126/science.1257594)
- Yang, E. J., J.-H. Hyun, D. Kim, J. Park, S.-H. Kang, H. C. Shin, and S. Lee. 2012. Mesoscale distribution of protozooplankton communities and their herbivory in the western Scotia Sea of the Southern Ocean during the austral spring. *J. Exp. Mar. Bio. Ecol.* **428**: 5–15. doi:[10.1016/j.jembe.2012.05.018](https://doi.org/10.1016/j.jembe.2012.05.018)
- Yebra, L., and others. 2018. Zooplankton production and carbon export flux in the western Alboran Sea gyre (SW Mediterranean). *Prog. Oceanogr.* **167**: 64–77. doi:[10.1016/j.pocean.2018.07.009](https://doi.org/10.1016/j.pocean.2018.07.009)
- Zhu, F., R. Massana, F. Not, D. Marie, and D. Vaultot. 2005. Mapping of picoeucaryotes in marine ecosystems with quantitative PCR of the 18S rRNA gene. *FEMS Microbiol. Ecol.* **52**: 79–92. doi:[10.1016/j.femsec.2004.10.006](https://doi.org/10.1016/j.femsec.2004.10.006)
- Zoccarato, L., A. Pallavicini, F. Cerino, S. Fonda Umani, and M. Celussi. 2016. Water mass dynamics shape Ross Sea protist communities in mesopelagic and bathypelagic layers. *Prog. Oceanogr.* **149**: 16–26. doi:[10.1016/j.pocean.2016.10.003](https://doi.org/10.1016/j.pocean.2016.10.003)

Acknowledgments

We sincerely thank the officers and crew of the *RRS James Clark Ross* for their logistical and technical support during the JR304 cruise, Anna Belcher (British Antarctic Survey) for sharing particulate organic carbon data, and Alison Baylay at the Environmental Genomics Facility (University of Southampton) for her assistance on next-generation sequencing. Funding support came from University of Southampton (Start-up Grant for Phyllis Lam) and the Natural Environment Research Council. We thank the reviewers for contributing to enhance the quality of this manuscript.

Conflict of Interest

None declared.

Submitted 28 January 2019

Revised 27 June 2019

Accepted 12 August 2019

Associate editor: David Walsh